



universität  
wien

# MASTERARBEIT / MASTER'S THESIS

Titel der Masterarbeit / Title of the Master's Thesis

„Effects of Transcranial Ultrasound Pulse Stimulation  
detected with fMRI“

verfasst von / submitted by

Gregor Dörl BSc BA

angestrebter akademischer Grad / in partial fulfilment of the requirements for the degree of  
Master of Science (MSc)

Wien, 2021 / Vienna 2021

Studienkennzahl lt. Studienblatt /  
degree programme code as it appears on  
the student record sheet:

A 066 834

Studienrichtung lt. Studienblatt /  
degree programme as it appears on  
the student record sheet:

Masterstudium Molekulare Biologie

Betreut von / Supervisor:

Ao. Univ.-Prof. Doz. Dr. Roland Beisteiner



## **Acknowledgments**

I would like to thank my supervisor Roland Beisteiner, for giving me the opportunity to write this thesis at his group. I am very glad for the support given and also the trust to work independently on parts of this paper.

I am also very grateful to my colleagues at the study group: Eva Matt, Benjamin Spurny-Dworak, Alina Domitner, Nejla Karahasanovic, Sonja Radjenovic, Anna Zettl, Lena Bender and everybody else, who make working at this group so very much enjoyable and have been an encouragement during tough times. Especially, I want to thank Eva Matt, who supported me so much during this project. She introduced me to fMRI data analysis and was always open for my questions, ideas or problems and had an answer at the ready. I also want to thank Benjamin Spurny-Dworak, who showed me (and still does) much about working in science.

Finally, I am truly thankful for my family and friends, who have given me support, inspiration and much happiness throughout the years of my study. Above all, I want to thank my wife Lea. She is my joy, my support and she makes every large obstacle appear much smaller.

## Abstract (en)

Ultrasound brain stimulation techniques have great potential for clinical application because of their non-invasiveness, as well as the possibility to precisely target regions-of-interest. Transcranial pulse stimulation (TPS) has been recently shown to be a safe and clinically viable stimulation technique. In a clinical sample with Alzheimer's Disease (AD) patients, 2-4 weeks of TPS therapy resulted in improved neuropsychological scores as well as functional connectivity (FC) as measured with functional magnetic resonance imaging (fMRI). In this study, an fMRI follow-up analysis is presented. Specifically, neuroplastic changes in FC due to TPS therapy and their potential behavioral correlates are explored.

Analyzing fMRI data showed a normalization of FC between the salience network (right anterior insula) and the ventromedial network (left frontal orbital cortex). This functional change correlated with improvements in depressive symptoms. Stimulation of brain areas related to depression (including the dorsolateral prefrontal cortex) with TPS may induce relevant functional changes and alleviate depressive symptoms.

TPS was previously hypothesized to induce location-dependent neuromodulatory effects. While AD patients showed overall cognitive improvements, visuo-constructive tests showed a decrease after TPS intervention. Notably, functionally relevant areas have been largely left out during stimulation. In this analysis, a matching decrease in FC measures of a visuo-constructive network is reported, further fortifying the claim of a location-dependent effect. Together, this study presents further evidence that TPS may become a beneficial clinical add-on therapy for neurological and psychiatric diseases.

## Abstract (de)

Hirnstimulation mit Ultraschall birgt viel Potential als eine klinische, nicht-invasive Stimulationstechnik, unter anderem aufgrund der Möglichkeit, präzise beliebige Hirnareale zu stimulieren. Transkranielle Pulsstimulation (TPS) ist eine sichere und klinisch anwendbare Stimulationsmethode. In einer ersten Untersuchung mit Alzheimerpatienten wurden nach 2-4 Wochen TPS Therapie Verbesserungen in neuropsychologischen Testwerten, sowie erhöhte funktionelle Konnektivität mittels funktioneller Magnetresonanztomographie (fMRT) festgestellt. Die vorliegende Untersuchung ist eine Folgeanalyse. Neuroplastische Veränderungen der funktionellen Konnektivität anhand von fMRT Daten und mögliche entsprechende neuropsychologische Veränderungen wurden erforscht.

In der ersten Analyse wurde eine Normalisierung der funktionellen Konnektivität zwischen dem Salience-Netzwerk (rechte anteriore Insula) und dem ventromedialen Netzwerk (linker frontoorbitaler Cortex) festgestellt. Diese funktionelle Veränderung korreliert mit Verbesserungen von depressiven Symptomen. Stimulation von Hirnarealen, die für Depression relevant sind (zum Beispiel der dorsolaterale Präfrontalcortex), mittels TPS verursacht möglicherweise relevante funktionelle Veränderungen und lindert depressive Symptome.

Es wird angenommen, dass TPS abhängig von dem Stimulationsort einen neuromodulatorischen Effekt hat. Zwar zeigten Alzheimerpatienten nach TPS Behandlung kognitive Verbesserungen, jedoch kam es zu einer Abnahme der visuo-konstruktiven Fähigkeiten. Funktionell relevante Hirnareale wurden während der Stimulation größtenteils ausgelassen. Die vorliegende Untersuchung zeigt eine entsprechende Verringerung von funktionellen Konnektivitätswerten eines visuo-konstruktiven Netzwerks, und untermauert die Hypothese der Effekte abhängig vom Stimulationsort. Zusammenfassend präsentiert diese Analyse weitere Belege, dass TPS eine nützliche ergänzende (add-on) Therapie für neurologische und psychiatrische Erkrankungen werden kann.

## Table of Contents

<b>Acknowledgments</b>	<b>3</b>
<b>Abstract (en)</b>	<b>4</b>
<b>Abstract (de)</b>	<b>5</b>
<b>1. Introduction</b>	<b>8</b>
<b>2. Methods</b>	<b>12</b>
2.1 Participants	12
2.2 Study design	12
2.3 TPS treatment and stimulation targets	12
2.4 Neuropsychological assessment	14
2.4.1 Depression scale	14
2.4.2 CERAD	14
2.5 MRI measurements	14
2.5.1 MRI parameters	15
2.5.2 Preprocessing	15
2.5.3 Preprocessing quality control	17
2.5.4.1 ROI-to-ROI-based connectivity	18
2.5.4.2 Graph theoretical analysis of a visuo-constructive network	19
2.5.4.3 Functional connectivity and behavior correlation	20
<b>3. Results</b>	<b>21</b>
3.1 Neuropsychological assessment	21
3.2 Functional connectivity analysis	22
3.2.1 ROI-to-ROI-based connectivity	22
3.2.1.1 FC analysis with Neurosynth	22
3.2.2 Graph theoretical analysis of visuo-constructive network	24

3.3. Correlation analysis .....	26
<b>4. Discussion .....</b>	<b>30</b>
4.1 Main findings .....	30
4.2 Functional connectivity changes correlate with improvements in depressive symptoms .....	30
4.3 Decreases in visuo-constructive neuropsychological scores and graph theoretical measures indicate location specific effects of TPS.....	32
4.4 Evidence for neuromodulatory and location dependent effects of TPS .....	35
4.5 Limitations and conclusion .....	37
<b>5. References.....</b>	<b>38</b>
<b>6. List of abbreviations .....</b>	<b>51</b>
<b>7. List of Figures and Tables .....</b>	<b>53</b>

## 1. Introduction

Alzheimer's disease (AD) represents the major cause of dementia in the current world population (Soria Lopez et al., 2019). As life expectancy in most countries continues to rise, AD will also increasingly become a central epidemiological problem. Dementia, a group of cognitive impairments that progress over time and cause substantial problems for daily activities (such as loss of episodic memory or trouble with orientation, both time and location wise), strongly impacts the life of patients and their relatives. Treatment options are still not able to substantially alter the course of the disease. Therefore, strategies to slow disease progression and maintain cognitive abilities for a longer period are of major importance to help patients as well as ameliorate the burden on relatives and health care systems (Lane et al., 2018). A particular interest lies in interventions suited for add-on therapy. AD has long been viewed as a multi-faceted disease with a diverse pathology and, therefore, different treatment strategies are required (Scheltens et al., 2016). Furthermore, as pharmacological treatments are not yet able to halt the degenerative etiology of the disease, clinical interventions that utilize cognitive reserve of a patient (and potentially show immediate effects on quality of life) are invaluable (Stern, 2012).

Non-invasive brain stimulation (NIBS) has been put forth to serve as a potential treatment for neurological (Camacho-Conde et al., 2021) and psychiatric diseases (Ferrarelli & Phillips, 2021). The most commonly used techniques are based on inducing an electric field in neural tissue using magnet coils, like transcranial magnetic stimulation (TMS; Hallett, 2000; Walsh & Cowey, 2000), or applying a current directly through the scalp, like transcranial direct current stimulation (tDCS; Caumo et al., 2012). It has been repeatedly shown that NIBS can be well combined with different neuroimaging techniques, like functional magnetic resonance imaging (fMRI), for both specifying optimal target sites as well as getting a functional readout of its effects (Bergmann et al., 2016). While TMS has already been approved for clinical application in major depressive disorder (MDD), there are clear limitations regarding spatial accuracy (Minjoli et al., 2017) or reaching deep brain tissue (Spagnolo et al., 2018).

Ultrasound (US) has been studied as a possible brain stimulation technique going back to experiments in the 1950s, where brain sonication was first reported to modulate brain activity in cats (Fry et al., 1958). After a time of low interest, it regained popularity with reports of low-intensity transcranial focused ultrasound (tFUS) eliciting neuron excitation

and motor responses in mice about a decade ago (Tufail et al., 2010). First experiments in humans followed a few years later, targeting mostly somatosensory and visual areas. Stimulation of somatosensory cortex elicited somatosensory evoked potentials and, furthermore, altered local electroencephalogram (EEG) oscillatory dynamics. Subjects also reported transient tactile sensations and performed better in sensory discrimination tasks (Legon et al., 2014; Mueller et al., 2014; Lee et al., 2015, 2016a). When targeting the visual cortex (V1), subjects reported phosphene perceptions. Changes in neural activity as measured by fMRI and EEG were also reported, specifically activation in visual cortex and visual network areas and visual evoked potentials, respectively (Lee et al., 2016b). The first clinical applications were in patients with disorders of consciousness. In a longitudinal study, a small group of patients with unresponsive wakefulness syndrome received global transcranial focused shockwave therapy 8-18 years after brain injury and showed symptomatic improvements (Lohse-Busch et al., 2014). While there were no sham controls, in the years prior to focussed pulse stimulation (with an unchanged regiment of basic complex therapy) there had not been any changes in vigilance in these patients. After intervention paired with ongoing basic therapy, all patients responded positively and had improved vigilance.

Two of the main advantages of US compared to electro-physiological brain stimulation techniques are its spatial specificity as well as the possibility to penetrate into the brain tissue and reach deep brain structures. One of the first examples of this in human subjects was a case report of a patient diagnosed with disorder of consciousness after severe brain injury, who received sonication from a single-element US transducer (Monti et al., 2016). While no sham control was conducted and only little physiological data provided, behavioral improvements and no adverse side effects were reported. Since then, several studies have targeted subcortical structures, such as unilateral thalamus (Legon et al., 2018; Badran et al., 2020), left basal ganglia (Cain et al., 2021a) and brainstem (Guerra et al., 2021). Sonication of the left unilateral sensory thalamus attenuated SEPs and decreased performance in a sensory discrimination task (Legon et al., 2018). Cain et al. (2021a) could show a decreased haemodynamic response from the targeted globus pallidus as well as a brain wide decrease in perfusion after stimulation with low-intensity focused US.

Besides the intriguing possibility to non-invasively influence brain structures in-vivo and directly observe functional implications (e.g. through behavior or imaging modalities), brain stimulation techniques are of particular interest as non-pharmacological treatment

alternatives. Animal models have long been used to study US stimulation as a possible treatment for disorders of the brain (Leinenga et al., 2016). While the first applications of US stimulation in human patients were in disorder of consciousness after severe brain injury (Lohse-Busch et al., 2014; Monti et al., 2016; Cain et al., 2021b), there is a wide field of possible applications. Psychiatric disorders are among the public health concerns in need of novel treatment options. The electro-physiological stimulation technique TMS is already FDA approved as a viable treatment option for major depressive disorder (e.g. reviewed in Perera et al., 2016). So far, there has only been one study that looked into US stimulation as a possible depression intervention in patients. In a sham controlled study, students suffering from mild to moderate depression did not show improvements on depression scales, but showed decreases in trait worry after receiving tFUS treatment (Reznik et al., 2020). Transcranial US to the right prefrontal cortex, a common target site for stimulation treatment in depression, showed improvements in mood and alterations in functional connectivity in healthy participants (Sanguinetti et al., 2020).

There are first reports of clinical efficacy of brain sonication in AD patients already receiving state-of-the-art treatment (Beisteiner et al., 2019; Jeong et al., 2021). Transcranial pulse stimulation (TPS) is a newly developed brain stimulation technique that generates ultra short pressure pulses to mechanically stimulate nerve tissue through the skull (Beisteiner et al., 2019). A first pioneering study applied pulse stimulation across the brain without navigation (Lohse-Busch et al., 2014). Here, individual brain images are generated with magnetic resonance imaging (MRI), so pulse stimulation can be precisely navigated in real-time. In a first clinical feasibility study, TPS has been shown to improve cognitive performance in 35 AD patients, specifically memory and verbal functions, for up to 3 months after intervention. Correspondingly, neuroplastic changes as measured by fMRI have also been reported. Beisteiner et al. (2019) showed increased functional connectivity (FC) in a memory network (Benoit & Schacter, 2015) during resting-state fMRI and task specific activation increase in the hippocampus after TPS intervention compared to a baseline session. Special structural MRI sequences also showed no major side effects. TPS has also been reported to reduce cortical atrophy in AD relevant areas (Popescu et al., 2021).

Two important aspects can be highlighted. Firstly, depression symptoms have also shown improvements after TPS treatment. Depression is a common co-morbidity in AD and particularly problematic as it increases the burden on patients and standard pharmacological intervention strategies are often limited (Galts et al., 2019). Thus, novel add-on treat-

ment options are needed. Secondly, AD patients in whom TPS was targeted to specific regions-of-interest (ROI) have shown a decline in visuo-constructive abilities over 3 months after treatment. Importantly, posterior and parietal regions, that are known to be involved in visuo-constructive processes (Serra et al., 2014), were not or only partially included in the stimulated ROIs. The decline was not observed in patients receiving global brain wide stimulation, so it was theorized to be due to a location specific effect of TPS. There are two aims of this fMRI follow-up analysis to Beisteiner et al. (2019). First, as depression symptoms have significantly improved after TPS therapy, potential changes in functional connectivity related to depression are investigated. Specifically, an ROI-to-ROI analysis was used to look for connectivity changes across the whole brain using a standard set of predefined ROIs. These FC changes were then correlated with individual depression scores to explore behavioral relevance. Secondly, according to the hypothesis of location specific stimulation effects, a related visuo-constructive functional network can be expected to show relative perturbations after TPS intervention that are also related to the decline in behavioral scores. Therefore, graph theoretical measures for a visuo-constructive network were examined. A decrease in connectivity measures is hypothesized.

## 2. Methods

### 2.1 Participants

For this study, a subgroup of a previously published report (Beisteiner et al., 2019), for which functional MRI data were available, was analyzed. This group consisted of 20 patients, who had been clinically diagnosed for AD according to criteria in ICD-10 (F00) and the National Institute of Aging-Alzheimer's Association criteria. Patient characteristics and relevant comorbidities can be found in Beisteiner et al. (2019). Briefly, most patients suffered from mild to moderate AD with a Mini-Mental State Examination (MMSE) score of  $\geq 18$ . However, an MMSE cutoff was not implemented to minimize inclusion criteria and better represent real world patient variability. The mean MMSE was 20.94, standard deviation (SD) was 5.8, range was 6-30. Common inclusion criteria were clinically stable patients with probable AD, optimized standard treatments, at least three months of stable antimentia therapy (if therapy was necessary), signed written informed consent, age  $\geq 18$  years. Common exclusion criteria were noncompliance with study protocol, relevant intracerebral pathology unrelated to AD (e.g. brain tumor), hemophilia or other blood clotting disorders or thrombosis, corticosteroid treatment within the last six weeks before first treatment, pregnant or breastfeeding women. After dropout, 18 patients completed the study and were used for further analysis.

### 2.2 Study design

The study design is summarized in Fig. 1. After successful inclusion, patients underwent neuropsychological testing as well as an initial MRI scan for anatomical data acquisition and baseline measurements. They then received TPS treatment for 4 weeks, with 3 sessions per week. Three patients only received TPS for 2 weeks and one patient for 3 weeks. After stimulation, patients underwent again neuropsychological testing and MRI measurements.

### 2.3 TPS treatment and stimulation targets

TPS treatment was applied using a NEUROLITH TPS generator (Storz Medical AG, Tägerwil, Switzerland). Single US pressure pulses with the following characteristics were applied: duration about 3  $\mu\text{s}$ , 0.2  $\text{mJ mm}^{-2}$  energy flux density, a maximum  $I_{\text{SPTA}}$  (spatial-peak-temporal-average intensity) of 0.1  $\text{W/cm}^2$ , pulse repetition frequency 5 Hz, 6000 pulses per therapeutic session. The brain areas targeted with TPS were defined by a neurologist and were chosen



**Figure 1: Diagram of the study design.** After successfully clearing screening, patients completed neuropsychological testing and resting-state fMRI recording for a baseline measurement. TPS stimulation was applied 3 times per week for 2-4 weeks, before another neuropsychological testing and fMRI measurement.

due to their relevance to AD. These regions of interest (ROIs), drawn in ellipsoid shape, include the dorsolateral prefrontal cortex (DLPFC) (a classical target in AD and depression brain stimulation; e.g. Pascual-Leone et al., 1996), areas of memory (including ROIs involved in the default mode network) and language networks. Anatomical scans were pre-evaluated to determine brain size variability (using an in-house software for gross estimation of the size of cerebrum), and one of two sets of standardized ROI sizes was employed, either for small or large sized patient brains. More specifically, ROIs comprised: bilateral frontal cortex (DLPFC and inferior frontal cortex extending to Broca’s area, ROI volume 136/164 cm<sup>3</sup> – 2 x 800 pulses per hemisphere), bilateral lateral parietal cortex (extending to Wernicke’s area, ROI volume 122/147 cm<sup>3</sup> – 2 x 400 pulses per hemisphere), and extended precuneus cortex (1 bilateral volume with 66/92 cm<sup>3</sup> – 2 x 600 pulses). During stimulation, the goal was to evenly distribute all pulses within the respective ROIs. NEUROLITH consists of a mobile single transducer and an infrared camera system, which tracks the patient’s head via goggles with infrared markers. Stimulation was administered equally over each ROI by adequate movement of the handpiece and tracked in real time to enable standardized distribution across the entire study group. To ensure proper pulse transmission, a large amount of bubble-free US gel was applied on skin and hair at the stimulation site. Further description is found in Beisteiner et al. (2019).

## **2.4 Neuropsychological assessment**

### **2.4.1 Depression scale**

To monitor effects of TPS on depressive symptoms, patients completed the Beck Depression Inventory (BDI-II) before beginning of therapy and after completing the whole cycle of treatment. After analyzing with a Kolmogorow-Smirnow-Test, test data was shown to not be normally distributed and were thus analyzed using the nonparametric Wilcoxon test for paired variables. Statistical analysis was done in SPSS 24 (IBM Corp. Released 2016. IBM SPSS Statistics for Windows, Version 24.0. Armonk, NY: IBM Corp.).

### **2.4.2 CERAD**

The German version of the CERAD Plus was used for testing (Ehrensperger et al., 2010). The CERAD raw scores were used to calculate the corrected total score (CTS; Chandler et al., 2005) for all subjects. Further, principle component analysis (PCA) scores were generated using the z-transformed scores (corrected for age, gender and formal education as performed by the CERAD Online analysis; norm population CERAD: N = 1100, phonemic word fluency N = 604). The PCA on the CERAD subtests produced statistically independent factors that were able to explain individual test performance with an eigenvalue > 1, and therefore allowed grouping subtests according to cognitive components for memory (MEMORY), verbal processing (VERBAL) and visuospatial or constructional processing (FIGURAL) scores (for a detailed description, see Beisteiner et al., 2019). Complete baseline and post stimulation test data was available for 16 patients. After testing FIGURAL test scores for normality and homoscedasticity with Shapiro-Wilk-Test and Levene-Test, respectively, data was shown to be normally distributed and thus a paired t-test was used.

## **2.5 MRI measurements**

To analyze functional changes in the brain from TPS intervention, resting-state fMRI data was collected. FMRI can measure very small magnetic changes in brain tissue due to metabolic activity corresponding to neural activity (Goebel, 2015). Blood-oxygenation level dependent (BOLD) contrast detects the vascular response to increased neural activity, which gives an indirect readout at a high spatial resolution (Ogawa et al., 1990). Measuring spontaneous brain activity when a subject is at rest has been shown to be highly structured across space and time (Pezzulo et al., 2021) and undergoes drastic changes in AD (Badhwar et al., 2017).

Consequently, it lends itself as a method to track functional changes related to disease progression as well as treatment efficacy (Hohenfeld et al., 2018).

### **2.5.1 MRI parameters**

MRI sequences were acquired with a 3 T SIEMENS PRISMA MR scanner with a 64-channel head coil. A T1-weighted structural image using an MPRAGE sequence (TE/TR = 2.7/1800 ms, inversion time = 900 ms, flip angle = 9°, resolution 1 mm isotropic) was recorded for navigation purposes. For functional images, a T2\*-weighted gradient-echo-planar imaging (EPI) sequence was used, with 38 slices aligned to AC-PC (anterior- and posterior-commissure), covering the whole brain including cerebellum (TE/TR = 30/2500 ms, flip angle = 90°, in-plane acceleration = GRAPPA 2, field of view = 230 x 230 mm, voxel size = 1.8 x 1.8 x 3 mm, 25% gap). 250 volumes (10 min 25 s total run time) for resting state fMRI were recorded. During scanning, patients were shown a white fixation cross on a black screen and were instructed to not move, let their thoughts roam freely and to not fall asleep.

### **2.5.2 Preprocessing**

In order to analyze recorded data, they need to undergo a number of preprocessing steps to get rid of noise and artifacts, as well as prepare for later statistical tests (Poldrack et al., 2011). All preprocessing procedures and subsequent analyses were performed using the CONN toolbox v19 (Whitfield-Gabrieli & Nieto-Castanon, 2012), which is an open-source software based on SPM12 (Wellcome Trust Centre for Neuroimaging; [www.fil.ion.ucl.ac.uk/spm/software/spm12](http://www.fil.ion.ucl.ac.uk/spm/software/spm12)).

First, images were realigned to the first scan of the first session by co-registering and resampling all subsequent subject scans. CONN employs the realign & unwarp procedure (Anderson et al., 2001) in SPM12, which combines a correction for head motion with a correction for distortions in the magnetic field of the scanner during acquisition. Second, images underwent a slice-time correction. Functional MRI scans only record one slice at a time, generating many 2-dimensional slices but at slightly different time points. To create a meaningful measure of brain activity at a single point in time, this inherent time-shift needs to be accounted for (Poldrack et al., 2011). CONN uses the SPM12 slice-timing correction procedure, as described by Henson et al. (1999), where a reference slice is chosen (time point in the middle of acquisition time) and data is then interpolated (using sinc interpolation) to match that slice. Third, potential outlier scans were corrected. Potential origins of such noisy out-

liers are, for example, severe subject motion or scanner drift and are being detected from the global BOLD signal and the amount of the subject's motion. An example is given in Fig. 2. After these preprocessing steps, additional denoising was performed to reduce residual noise and variability factors from non-neural origins. Particularly in functional connectivity analyses these steps receive considerable importance, as residual noise factors may introduce strong biases (Poldrack et al., 2011). 12 potential confounding motion effects were identified and removed. These comprise 3 translation and 3 rotation motion parameters as well as their respective first-order derivatives. Further, an anatomical component-based noise correction method (aCompCor) was applied (Behzadi et al., 2007). This procedure derives 5 noise components each from cerebral white matter and with CSF areas, which are known to introduce non-neural signal, and are then included in the final regression model. In another scrubbing step, previously identified outlier scans were removed, a total of 101 parameters. Lastly, a filter with a pass band of 0.008 to 0.09 Hz was applied after regression to avoid a mismatch in frequencies between signal and nuisance regressors (Hallquist et al., 2013). As the most important signal in fMRI is in slow-frequency fluctuations, filtering helps to reduce noise outside this frequency range, which is most likely of non-neural origin.

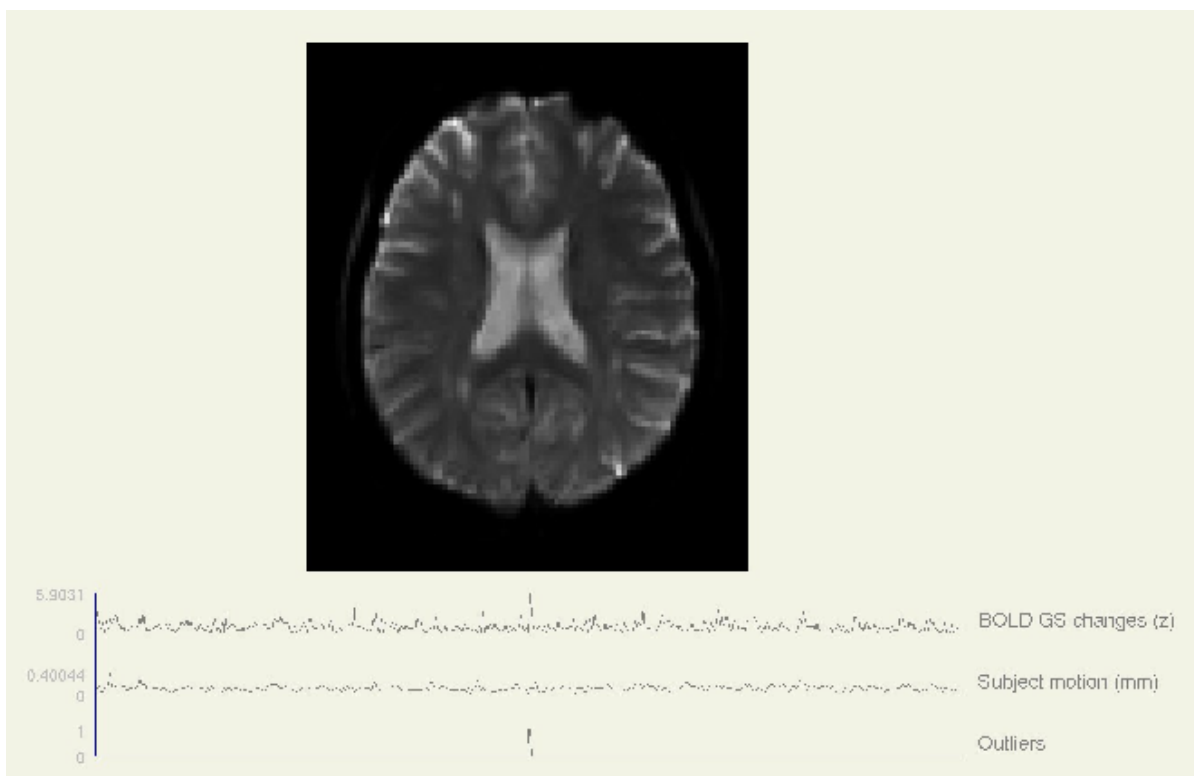


**Figure 2: Example of outlier detection (subject 18).** The observed global BOLD signal combined with the amount of subject-motion returns a potential outlier, which in turn is used as a possible confounding effect in a later denoising step to remove its influence on the signal.

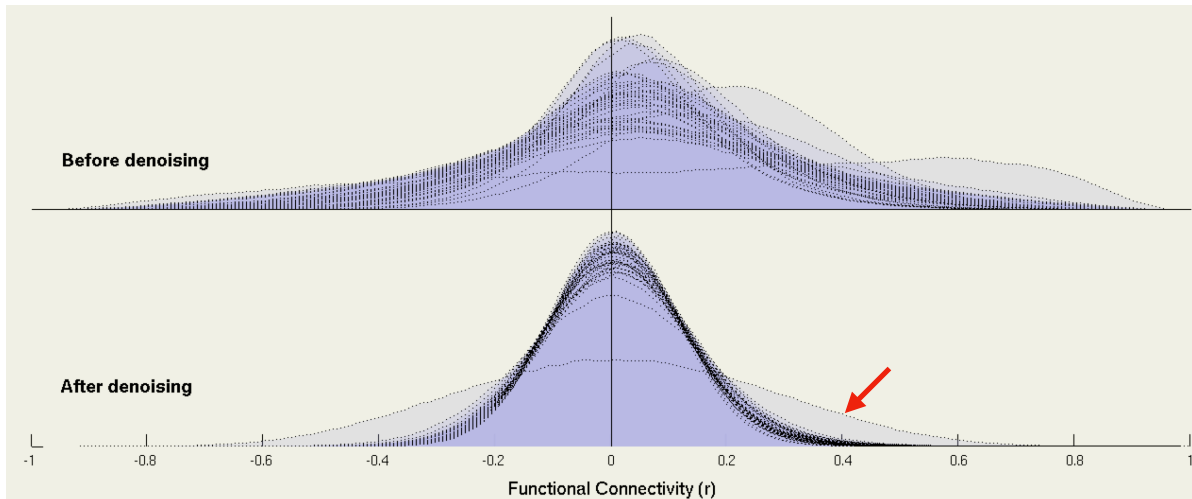


**Figure 3: FC distribution before and after denoising procedures.** Correlations between pairs of randomly connected points in the brain before denoising show a biased and spread distribution. After denoising, distribution is much more normally distributed. Red arrow indicates distribution for subject 01, which still shows a large spread after denoising and is not included in final analysis.

### 2.5.3 Preprocessing quality control

To assure proper preprocessing and denoising output, several quality controls were checked during and after the procedures described above. Successful denoising was controlled by estimating pairs of FC values between randomly selected points in the brain and evaluating the resulting distribution of FC values. This was done before and after the denoising procedures were applied (Fig. 3). Note that after denoising, distributions of FC values are much more resembling a Gaussian shape and have smaller tails, i.e. randomly selected points have less correlation bias. Further note, that data from subject 01, where FC distribution still shows a flat curve and very long tails (Fig. 3, indicated by red arrow), was excluded from further analysis.

As another quality check, QC-FC correlations were computed and evaluated, as described by Ciric et al. (2017). This procedure calculates FC values between pairs of random points in the brain and correlates them with 5 quality-control (QC) measures (e.g. subject motion, BOLD signal z-score changes). These measures are calculated before and after denoising steps and summarized in a distribution of QC-FC correlations. As presented in Fig. 4, denoising shifted QC-FC correlation values more towards the expected distribution (indicated by the red-dashed line).

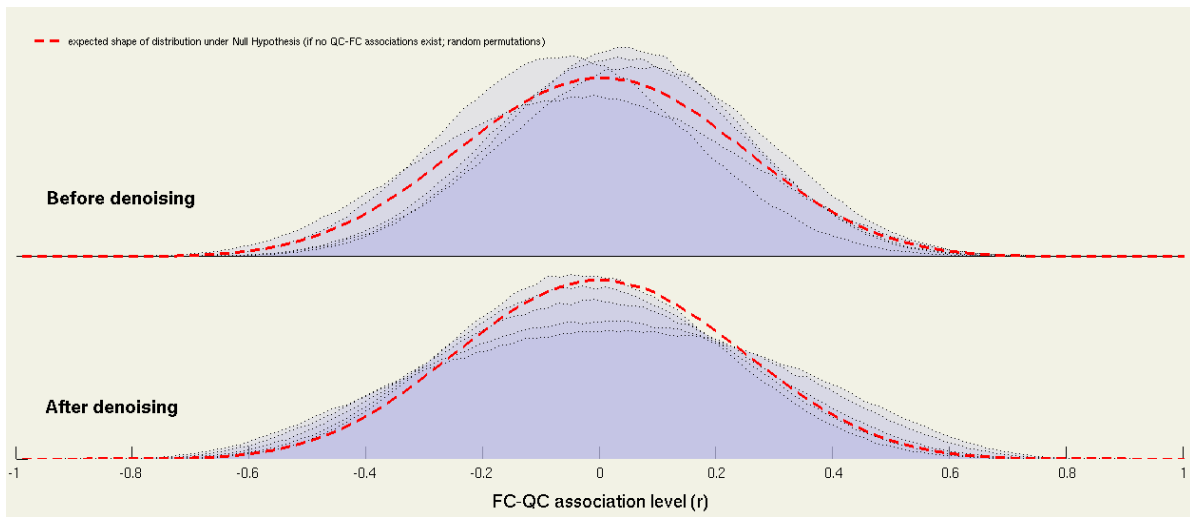


**Figure 4: QC-FC correlation distribution before and after denoising.** Distribution of calculated QC-FC correlation values is closer to expected null hypothesis of no QC-FC associations. Red dashed line indicates the expected distribution.

#### 2.5.4 Functional connectivity analysis

For a further group analysis, bivariate correlations between each pair of ROIs were calculated on a subject level, weighted for each pre and post stimulation sessions and further Fisher-transformed to a Z-score matrix. This generates a single statistical parametric map with one T- or F-value for each voxel and gives information on the connectivity (Whitfield-Gabrieli & Nieto-Castanon, 2012).

##### 2.5.4.1 ROI-to-ROI-based connectivity

For the subsequent group analysis, all 164 default ROIs in the CONN toolbox were chosen, which include cortical and subcortical ROIs according to the Harvard-Oxford atlas and predefined CONN toolbox network ROIs that are derived from ICA analyses of the HCP dataset. The post stimulation session was compared to the pre stimulation baseline using the connection threshold 0.05 p-FDR (False discovery rate) corrected, combined with a multi-voxel pattern analysis (MVPA) omnibus test (cluster threshold 0.05 p-uncorrected) on ROI-level. The MVPA omnibus test represents a multivariate test measure which characterizes the strength of all effects or connections from each ROI.

#### 2.5.4.2 Graph theoretical analysis of a visuo-constructive network

Graph theoretical measures were calculated within an a priori defined network. This visuo-constructive network was chosen from Serra et al. (2014), where volumetric grey matter reduction in AD patients with visual constructional deficits was compared to AD patients without such deficits. The reported visuo-constructive network (VisNW) was largely in posterior and parietal brain areas and comprised the bilateral Angular gyrus (AG L, AG R), right intracalcarine cortex (ICC R), right posterior medial temporal gyrus (pMTG R), posterior cingulate cortex (PCC) and right temporo-occipital fusiform cortex (toFusC R) (Tab. 1). Further, the reported network included the precuneus (Precun). As this particular ROI was also among the targeted ROIs during TPS therapy, the first network analysis was conducted without the Precun to account for a potential effect from stimulation. In a second analysis, the Precun was included to explore this putative confound (VisNW+Precun). The corresponding location of the ROIs in the Harvard-Oxford atlas, which is implemented in CONN, was checked visually using FSLeyes.

These ROIs were defined in a nondirectional graph as nodes, with supra-threshold connections as edges. For each subject and condition, a graph adjacency matrix was then computed and compared between post stimulation and baseline. For the adjacency matrix a correlation coefficient of 0.35 was chosen as threshold to define connected ROIs. For the analysis threshold,  $p = 0.05$  FDR-corrected and a two-sided, paired t-test was chosen.

**Table 1: List of ROIs for graph analysis of a visuo-constructive network**

	<b>ROI</b>	<b>abbr.</b>	<b>Hemisphere</b>	
<b>Visuo-constructive NW</b>	Angular gyrus	AG L, AG R	bilateral	
	Intracalcarine cortex	ICC R	right	
	Posterior medial temporal gyrus	pMTG R	right	
	Posterior cingulate cortex	PCC	bilateral	
	Temporo-occipital fusiform cortex	toFusC R	right	
	<i>Precuneus</i>	<i>Precun</i>	<i>bilateral</i>	<i>included in VisNW+Precun</i>

Global efficiency (GE) is defined as inverse of the average shortest path between a particular node and all other nodes in the same graph (Achard & Bullmore, 2007). GE represents a degree of global connectedness of each ROI within a network. For a network, GE can be understood as a measure of inter-connectedness of the entire network and the capacity for parallel processing, contrasted with e.g. a higher GE in a random graph. The betweenness centrality (BC) is the fraction of shortest paths that pass through a particular node. In other words, it is the proportion of times that a node is part of a shortest path in the network. BC indicates the control of information flow which passes through the node (Sporns, 2011). Lastly, degree (Dg) is the number of edges from and to each node. Cost (Ct), which is the inverse of Dg, represents the proportion thereof. These two measures characterize the level of local connectedness of an ROI within a network (Nieto-Castanon, 2020).

#### *2.5.4.3 Functional connectivity and behavior correlation*

Individual FC values of significant ROI-to-ROI connections (post stimulation vs. baseline) were correlated with BDI-II scores using non-parametric Spearman rank correlation analysis. Equally, GE measures for VisNW and VisNW+Precun were correlated with CERAD CTS, MEMORY, VERBAL and FIGURAL scores, also using non-parametric Spearman rank correlation. Computations were performed in R (R Core Team (2020). R: A language and environment for statistical computing. R Foundation for Statistical Computing, Vienna, Austria. URL <https://www.R-project.org/>).

### 3. Results

#### 3.1 Neuropsychological assessment

14 out of 18 patients completed the BDI-II questionnaires in both sessions and could be included. The mean BDI-II score was 7.36 (SD = 5.09) at baseline and 5.00 (SD = 4.11) in post stimulation session, indicating mild depression symptoms as is common in AD (Galts et al., 2019). Comparing the two sessions using the non-parametric Wilcoxon-Test showed a significant improvement after TPS therapy ( $p = 0.037$ , two-tailed; Fig. 5).

As previously reported (Beisteiner et al., 2019), the CERAD CTS showed significant improvement in the cognitive state after treatment. For 16 out of 18 patients, the PCA factor loadings could be taken to divide CERAD subtest results into MEMORY, VERBAL and FIGURAL factors. FIGURAL scores showed a tendency to decline after stimulation ( $p = 0.0558$ ; Fig. 6). Notably, this decline was significant 3 months after stimulation (Beisteiner et al., 2019).

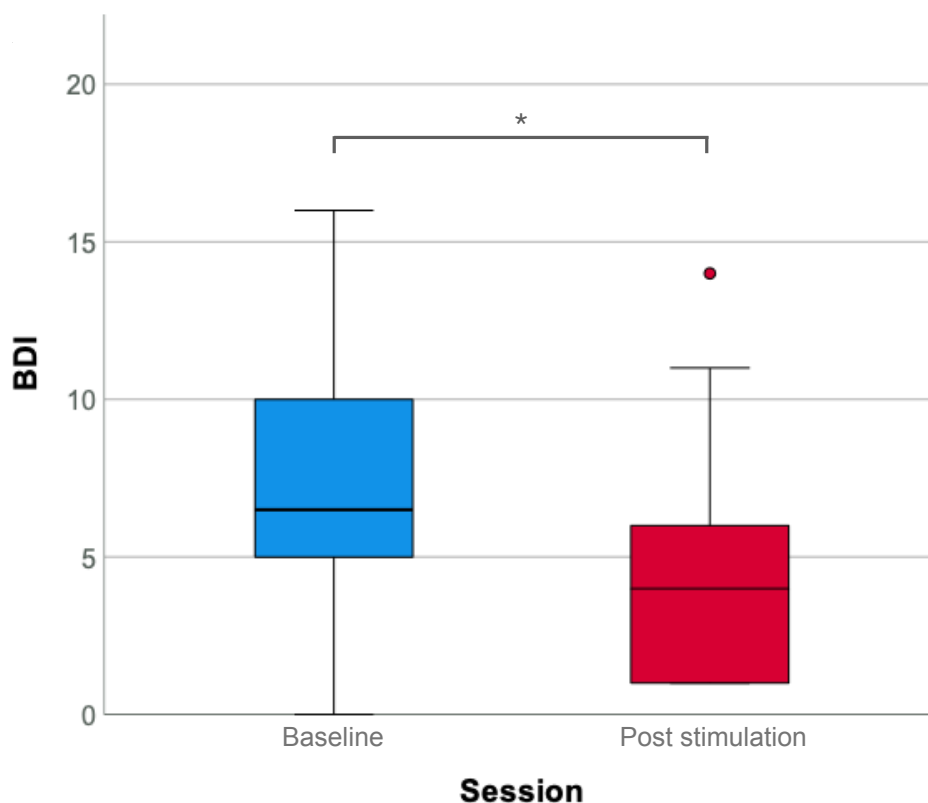


**Figure 5: Improvement of depression score (Beck Depression Inventory, BDI-II) after TPS stimulation.** Comparing the BDI-II depression score (N = 14) at baseline and after TPS stimulation with paired Wilcoxon-Test showed a significant improvement after TPS therapy.

\*  $p < 0.05$

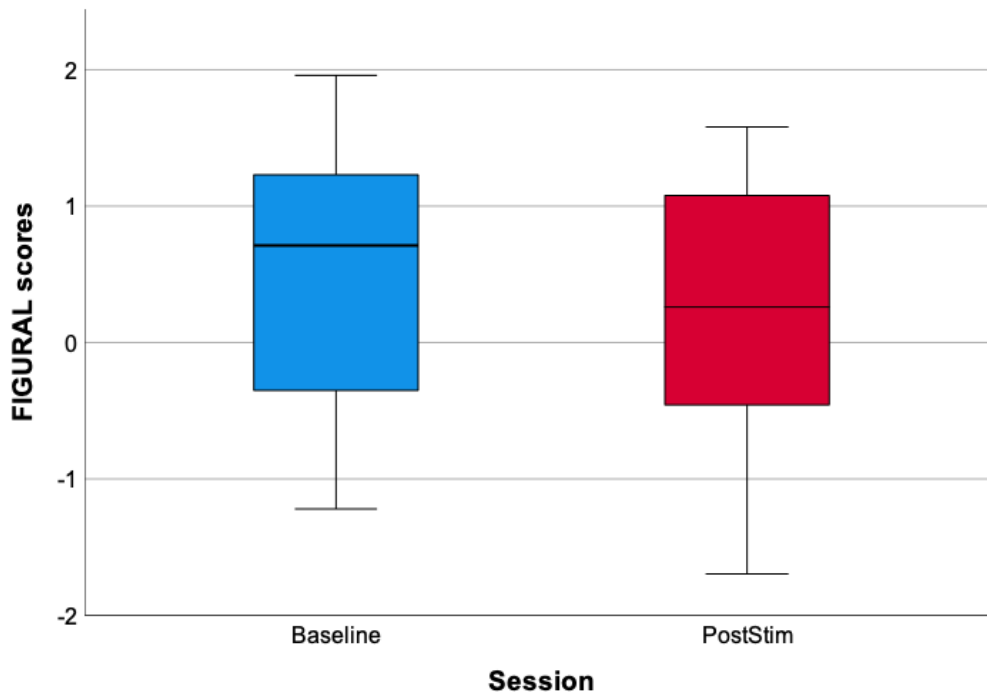


**Figure 6: FIGURAL test scores show a tendency to decline after TPS therapy.** Comparing the CERAD FIGURAL scores at baseline and after TPS stimulation with a paired t-test showed a tendency to decline, slightly below significance ( $p = 0.0558$ ;  $N = 16$ ).

## 3.2 Functional connectivity analysis

### 3.2.1 ROI-to-ROI-based connectivity

ROI-to-ROI FC analysis revealed a significantly lower FC between the left frontal orbital cortex (FORb L) and the right anterior insula (AInsula R) (Fig. 7). The latter represents a part of the salience network as defined by the CONN toolbox. Interestingly, all patients displayed a positive FC between FORb L and AInsula R at baseline (Fig. 8).

#### 3.2.1.1 FC analysis with Neurosynth

The online meta-analysis tool Neurosynth (Yarkoni et al., 2011) was used to further investigate FC characteristics between FORb L and AInsula R. Neurosynth is based on resting-state FC data of 1000 healthy subjects. This allows for a basic estimation of a typical physiological FC in healthy adults. Inspecting the FC map of the FORb L (MNI coordinates  $X = -44$ ,  $Y = 34$ ,  $Z = -12$ ) revealed a negative FC to the AInsula R (MNI coordinates  $X = 38$ ,  $Y = 18$ ,  $Z = 8$ ), specifically with a peak FC value of  $r = -0.24$  (Fig. 9). This is markedly different to the observed FC in the patient sample (Fig. 8).

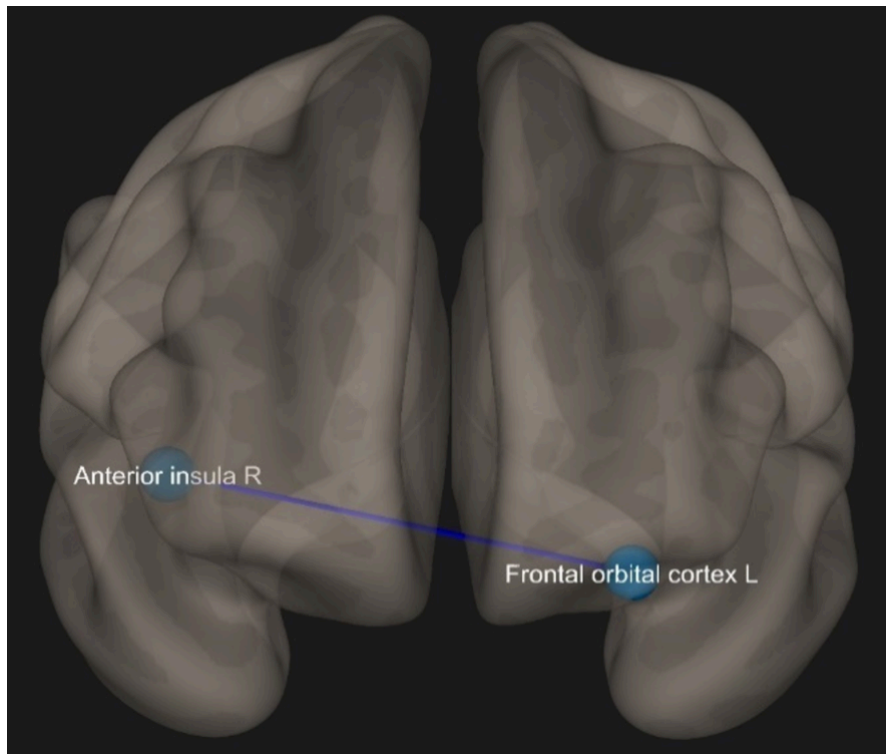


**Figure 7: Functional connectivity changes following TPS treatment in ROI-to-ROI connectivity analysis.** ROI-to-ROI-based FC analysis showed a significantly lower FC between the left frontal orbital cortex and the right anterior insula (part of the salience network) comparing the post stimulation session to the baseline session.

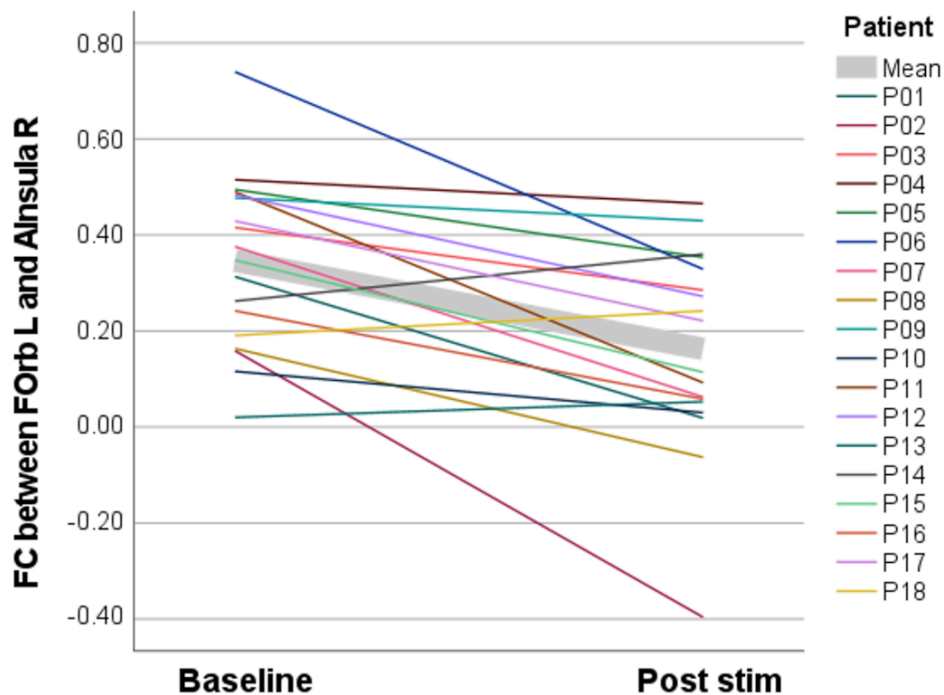


**Figure 8: Individual FC values between left frontal orbital cortex (FOrb L) and right anterior insula (AInsula R) at baseline and post stimulation sessions.** FC values are positive at baseline for every individual, while the average FC change decreased after TPS intervention (15 out of 18 patients). Each individual is indicated by a different color; the average FC change is indicated by the bold grey line.

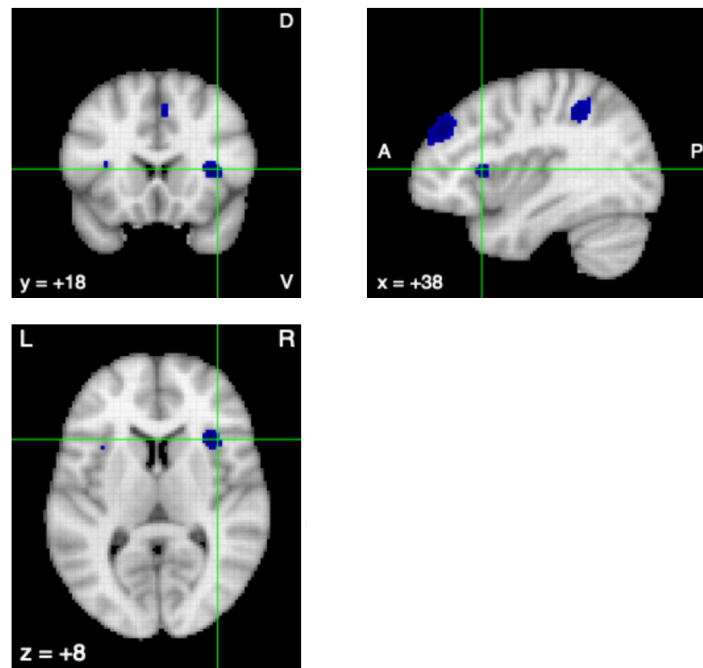


**Figure 9: Functional connectivity map derived from Neurosynth (Yarkoni et al., 2011) shows negative connectivity between FOrb L and AInsula R.** Neurosynth is an online meta-analysis tool using resting-state FC data from 1000 individuals. FOrb L (MNI coordinates  $X = -44$ ,  $Y = 34$ ,  $Z = -12$ ) shows negative connectivity with AInsula R (shown in image; MNI coordinates  $X = 38$ ,  $Y = 18$ ,  $Z = 8$ ) with a peak value of  $r = -0.24$ .

### 3.2.2 Graph theoretical analysis of visuo-constructive network

Analyzing the VisNW post vs. pre stimulation revealed a decrease in GE for the AG R ( $p$ -FDR = 0.0153; Fig. 10), a decrease in BC for AG R ( $p$ -FDR = 0.0416), as well as a decrease in Ct (and Dg) for AG R ( $p$ -FDR = 0.0272) and ICC R ( $p$ -FDR = 0.0459) (Tab. 2). Analyzing the individual connectivity values revealed that only a minority (2 out of 18 individuals) had a small increase in GE for the AG R (Fig. 11). In all the graph theoretical measures mentioned above, the whole network also tended to decrease but the values did not survive FDR-correction.

The individual GE values for the AG R paired with the corresponding FIGURAL scores show the overall expected trend of a joint decrease (Fig. 12). Note, while there was variance in the response pattern, only 3 individuals went visibly against the expected orientation and displayed a decrease in GE while having a higher FIGURAL score post stimulation.

For the VisNW+Precun, only GE ( $p$ -FDR = 0.0262) and Ct (and Dg) ( $p$ -FDR = 0.0147) for AG R decreases post vs. pre stimulation (Tab. 2).

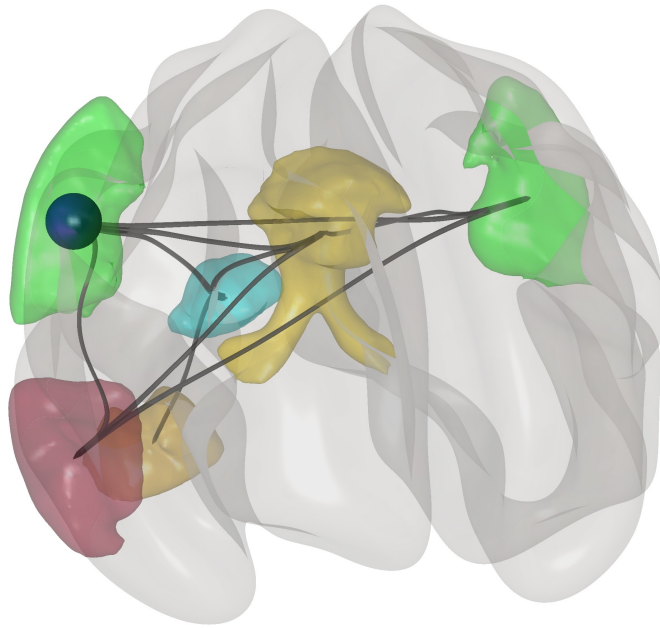


**Figure 10: Visuo-constructive network shows reduced global efficiency (GE) post vs. pre stimulation.** Graph theory analysis shows significantly reduced GE (indicated by the blue sphere) in the right angular gyrus, a hub in the network described by Serra et al. (2014). The angular gyrus (bilateral) is shown in green, posterior cingulate cortex in yellow, right intracalcarine cortex in blue, right posterior medial temporal gyrus in red and right temporo-occipital fusiform cortex in orange.

**Table 2: Graph measures post vs. pre stimulation for two visuo-constructive networks**

	ROI	Global Efficiency		Betweenness Centrality		Cost (and Degree)	
		p	T	p	T	p	T
<b>VisNW</b>	Whole network	<i>0.016</i>	-2.66			<i>0.0332</i>	-2.32
	Angular gyrus right	0.0153*	-3.53	0.0416*	-3.07	<i>0.0272</i>	-3.18
	Intracalcarine cortex right					0.0459*	-2.61
<b>VisNW+Precun</b>	Angular gyrus right	0.0262*	-3.36			0.0147*	-3.55

\* indicates significance after FDR correction; the uncorrected p-value (when it did not survive FDR-correction) is in italics

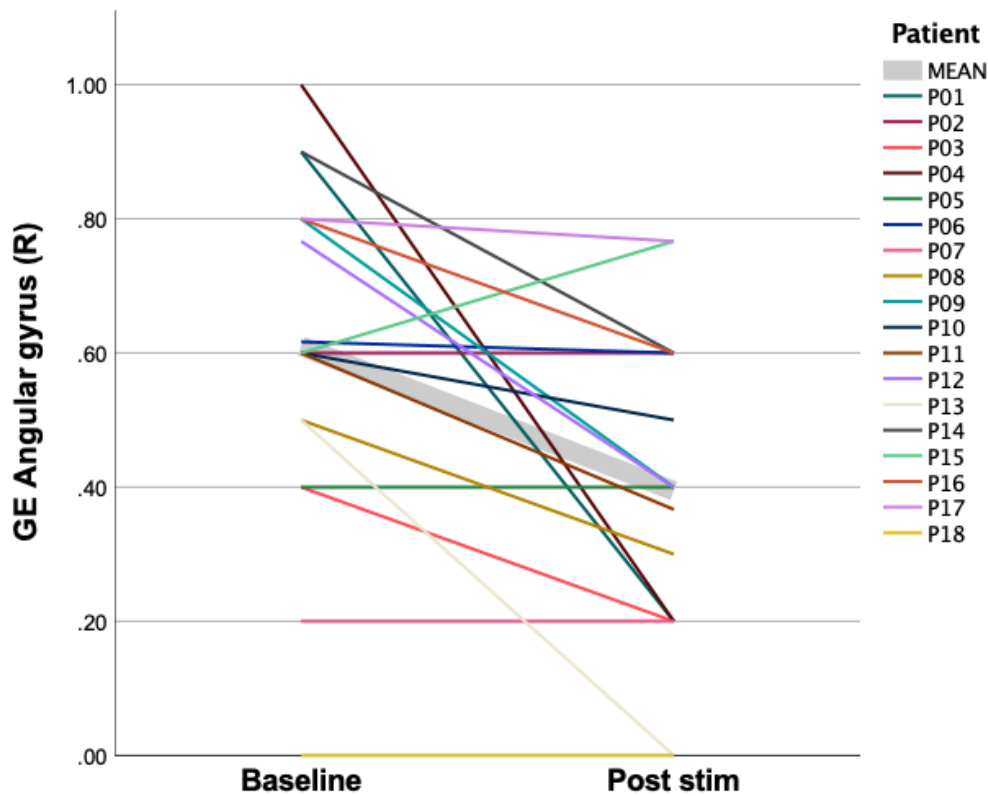


**Figure 11: Individual global efficiency (GE) values for the right angular gyrus (AG R) at baseline and post stimulation session.** Comparing post stimulation with the baseline session shows either a decrease or no change in GE for the AG R for the majority of individuals (16 out of 18 patients). Each individual is indicated by a different color; the average GE change is indicated by the bold gray line.

### 3.3. Correlation analysis

Individual FC values between FOrb L and Alnsula R post stimulation positively correlated with matching BDI-II scores ( $\rho = 0.541$ ,  $p = 0.046$ ,  $N = 14$ ; Fig. 13). Lower FC values corresponded to lower BDI-II scores, i.e. better improvements of depressive symptoms.

Individual GE values from the whole VisNW positively correlated with the pooled (CERAD) FIGURAL scores. All nodes, except for PCC and toFusC R also correlated with the FIGURAL scores. Additionally, pMTG R also correlated with CTS scores (Fig. 14). GE values from is NW+Precun showed a tendency to correlate less strongly with FIGURAL scores. However, GE of the whole network, pMTG R, PCC and Precun correlated also with CTS scores (Fig. 15). When dividing the GE of the whole VisNW and FIGURAL measurements into baseline and post stimulation session, Spearman's  $\rho$  still shows a positive correlation but loses significance (Baseline:  $\rho = 0.386$ ,  $p = 0.14$ ,  $N = 16$ ; Post Stimulation:  $\rho = 0.411$ ,  $p = 0.114$ ,  $N = 16$ ; Fig. 16).

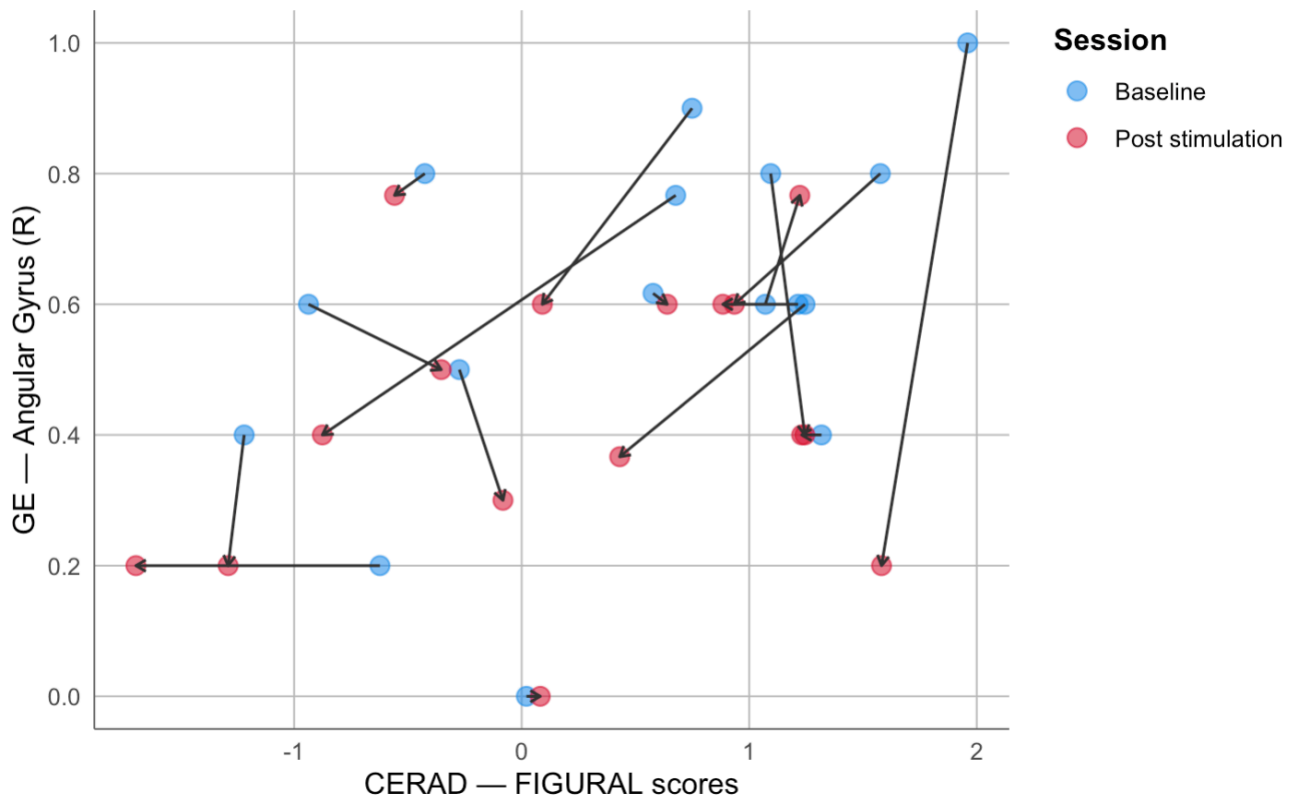


**Figure 12: Decrease in global efficiency (GE) in the right angular gyrus (AG R) corresponds to a decline in visuo-constructive test scores.** Individual values from the baseline and post stimulation session show that the majority of decreased GE in the AG R went hand in hand with a decline in FIGURAL scores. One subject showed an increase in both GE and FIGURAL scores (along the expected direction of the relationship) and only three subjects visibly displayed a large decline in GE paired with a slight increase in behavioral test performance. Arrows indicate individual values paired across both sessions.

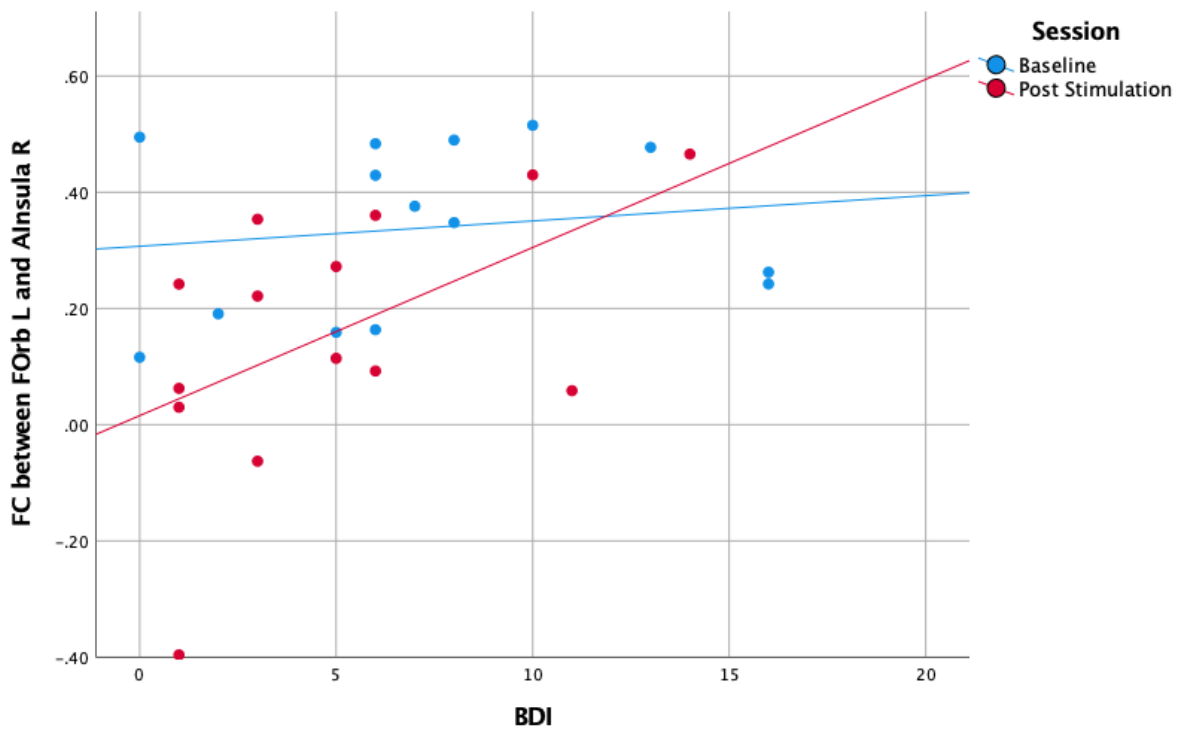


**Figure 13: Functional connectivity post stimulation correlates with depression symptom improvements.** BDI-II scores post TPS intervention correlate to ROI-to-ROI connectivity changes between left frontal orbital cortex (FOrb L) and right anterior insula (AInsula R). Individual data points for baseline session are in blue, for post stimulation session in red with fitted lines. The significant positive correlation post stimulation ( $\rho = 0.541$ ,  $p = 0.046$ ,  $N = 14$ ) indicates that lowered connectivity between these ROIs corresponded to better improvements in depressive symptoms.

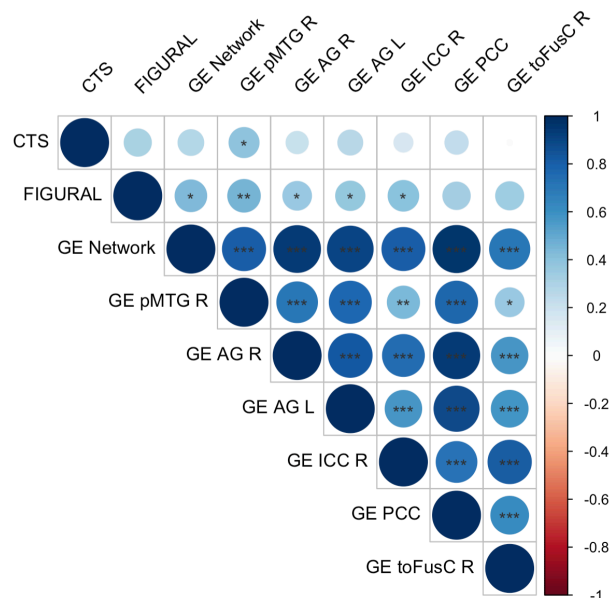


**Figure 14: Global efficiency (GE) for visuo-constructive network (without precuneus) correlates with (CERAD) FIGURAL scores.** Pooled GE of whole network correlates primarily with FIGURAL test scores ( $N = 32$ ). CTS stands for (CERAD) corrected total score, pMTG R for right posterior middle temporal gyrus, AG R/L for right/left angular gyrus, ICC R for right intracalcarine cortex, PCC for posterior cingulate cortex and toFusC R for right temporo-occipital fusiform cortex.

\*  $p < 0.05$ ; \*\*  $p < 0.01$ ; \*\*\*  $p < 0.001$

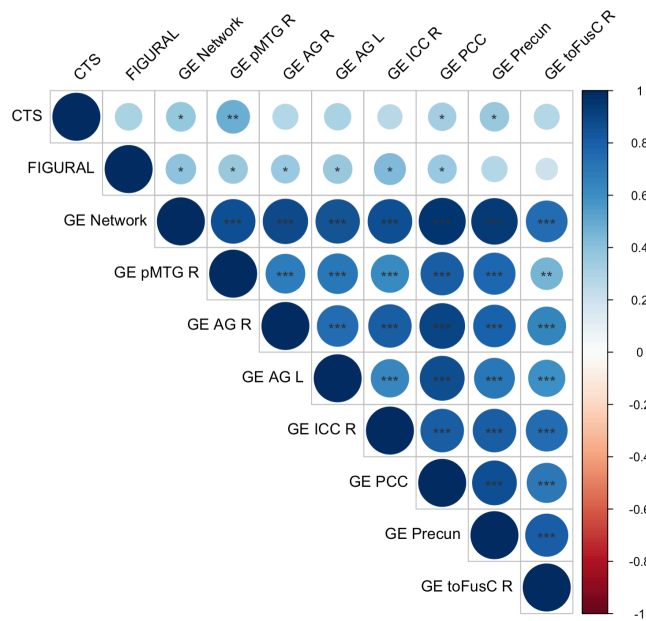


**Figure 15: Global efficiency (GE) for visuo-constructive network (including precuneus) correlates with (CERAD) FIGURAL and CTS scores.** Pooled GE of whole network correlates with FIGURAL test scores, but also to an extent with global CTS (N = 32). CTS stands for (CERAD) corrected total score, pMTG R for right posterior middle temporal gyrus, AG R/L for right/left angular gyrus, ICC R for right intracalcarine cortex, PCC for posterior cingulate cortex, Precun for precuneus and toFusC R for right temporo-occipital fusiform cortex.  
 \* p < 0.05; \*\* p < 0.01; \*\*\* p < 0.001

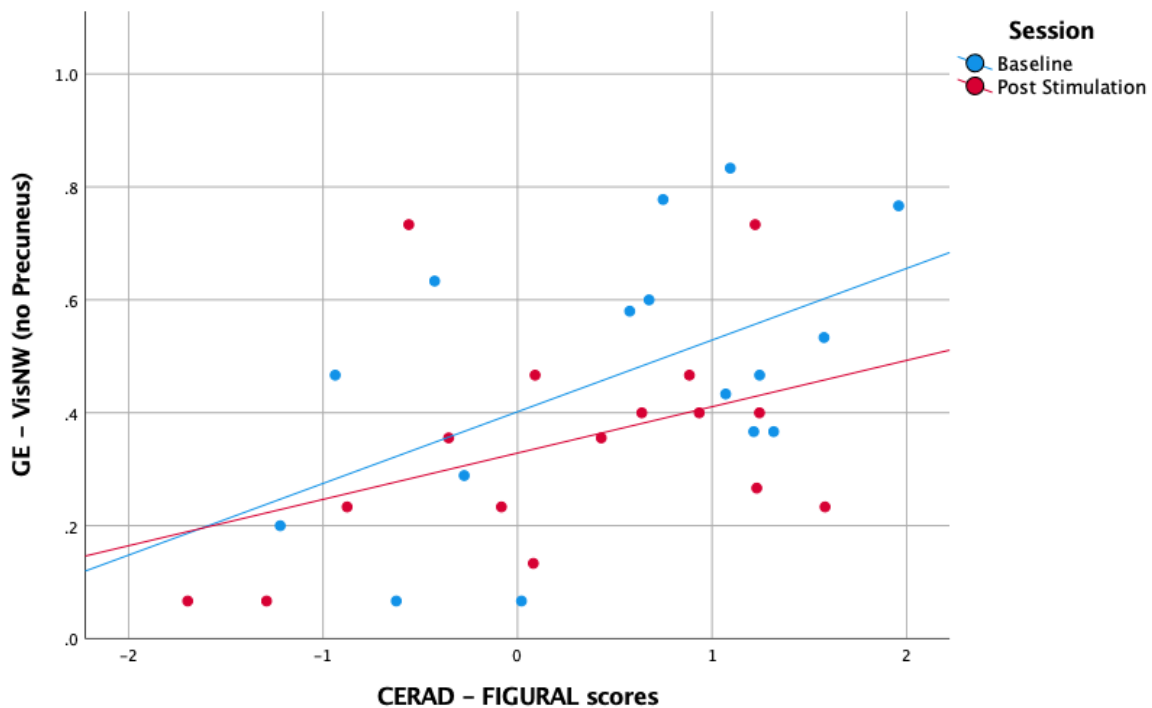


**Figure 16: Global efficiency (GE) of visuo-constructive network and (CERAD) FIGURAL scores at baseline and post TPS intervention show a joint trend.** Correlating pre and post GE of a visuo-constructive network with FIGURAL test scores shows a non-significant trend towards a positive correlation (Baseline: Spearman's rho = 0.386, p = 0.14, N = 16; Post Stimulation: Spearman's rho = 0.411, p = 0.114, N = 16). VisNW stands for visuo-constructive network, excluding the precuneus.

## 4. Discussion

### 4.1 Main findings

The aim of the current study was to further investigate effects of clinical TPS therapy in a small AD patient cohort as detected by resting-state fMRI, as a follow-up study to Beisteiner et al. (2019). Complementing these analyses are neuropsychological assessments which have shown significant changes after TPS. The main findings of this analysis are twofold.

First, a significant decrease in FC between the FOrb L and AInsula R was shown. Crucially, this change from a positive towards negative FC approached the expected, physiological anti-correlation. Correspondingly, lower FC correlated with more improved depressive symptoms, indicating a functional basis for this behavioral change.

Secondly, matching an initially reported decline in visuo-constructive scores, we show a decrease in connectivity measures of a VisNW. These behavioral changes have been previously proposed as a sign for location specific effects of TPS, because functionally related areas have been mostly omitted during stimulation. The decline in connectivity, shown here, reinforces this hypothesis.

### 4.2 Functional connectivity changes correlate with improvements in depressive symptoms

Comparing post stimulation vs. baseline, resting-state fMRI data revealed a significant decrease in FC between the FOrb L and AInsula R. The overall connectivity values correlated with BDI-II in AD patients. Lower FC between FOrb L and AInsula R after TPS intervention corresponded to better improvements in depressive symptoms (Fig. 13). FOrb L and AInsula R represent two nodes of the ventromedial network (VMN) and the salience network (SN), respectively (Dunlop et al., 2017; Seeley, 2019). In a comprehensive network analysis, Dunlop et al. (2017) have demonstrated the VMN and SN to be anti-networks, i.e. negatively correlated networks. Accordingly, an analysis using Neurosynth (Yarkoni et al., 2011) revealed a negative correlation between FOrb L and AInsula R, two central hubs of these respective networks. In contrast, the results presented here show that individual FC values between FOrb L and AInsula are positive in all patients before TPS intervention and approach a more negative connectivity after stimulation (Fig. 8). This suggests a pathological FC between the two network nodes, presumably due to AD effects on FC architecture. AD has widespread disturbing effects on functional network

connectivity in the brain (Agosta et al., 2012). A possible hypothesis is therefore that due to AD depression the negative correlation between these areas was disrupted in the patient cohort but improved after TPS.

Current understanding of resting-state FC in depression is still incomplete (Brakowski et al., 2017) and even more so in depression as a comorbidity in AD (Kim & Kim, 2021). MDD has been linked to hypoactivity in the SN and hyperactivity in the VMN (Koenigs & Grafman, 2009). During resting-state measurements, MDD patients show reduced activation in central nodes of the SN (Dunlop et al., 2017). Furthermore, responses to anti-depressive electrical brain stimulation treatments were associated with frontal cortical and limbic brain regions. For instance, the subgenual anterior cingulate cortex (sgACC), another node of the SN, is implicated in several studies analyzing the efficacy of repeated TMS (Dichter et al., 2015). Specifically, hyperconnectivity between the sgACC with the default mode network and central control network predicted the degree of symptom improvement after repeated TMS (Liston et al., 2014). Fox et al. (2012) showed that the efficacy of the TMS target site at the DLPFC is positively correlated with the degree of functional anticorrelation the target site has with the sgACC.

Depression is one of the most common neuropsychiatric comorbidities of AD (Zhao et al., 2016). Pharmacological therapies have shown limited to no effects of standard antidepressant therapy, such as selective serotonin reuptake inhibitors, in AD patients (Banerjee et al., 2013) and understanding of the molecular basis of depression in AD is still incomplete (Siarkos et al., 2015). There are non-pharmacological alternatives that have been shown to have positive effects on depression in dementia. Such strategies include, for instance, music therapy or reminiscence therapy, i.e. recalling and telling stories (Abraha et al., 2017). Further, while there are mixed reports concerning effects of physical therapy, a physically active lifestyle can decrease risk in dementia and MDD (Mammen & Faulkner, 2013; Rovio et al., 2005). Overall, there is still a need for novel therapeutical interventions to ameliorate depression in AD, as well as generally in MDD.

Several studies have now shown that brain stimulation using US may become a potential add-on therapy for depression. Sanguinetti et al. (2020) showed that tFUS to the right inferior frontal gyrus (IFG R) could improve mood in healthy subjects, as well as changes in FC. Specifically, a decrease in FC between the IFG R and the sgACC and FOrb was reported. Reznik et al. (2020) showed an effect of tFUS to the right frontotemporal cortex on the mitigation of worry in college students with mild to moderate depression. Besides these preliminary results in human subjects, there is also evidence present for animal

models. In a rat depression model, 15 min/day low-intensity tFUS for 2 weeks could reverse the depressive phenotype (anhedonia, tested by sucrose preference test, as well as exploratory behavior; Zhang et al., 2019). Furthermore, hippocampal brain-derived neurotrophic factor (BDNF) was increased compared to sham stimulated rats, indicating neuroplastic effects of stimulation. Notably, decreased BDNF levels have been shown consistently in patients with depression and have been suggested as a potential biomarker for disease activity (Fernandes et al., 2015). In a different rat depression model, Zhang et al. (2020) could show that tFUS stimulation to the ventromedial prefrontal cortex in awake rats also improved depression-like behaviors (sucrose preference) and enhanced BDNF in the prefrontal cortex compared to depressed control rats.

The results presented here show the first evidence for treating depressive symptoms in AD patients in a clinical study using a brain sonication technique. Together with global cognitive improvements and FC improvements in a memory network (Beisteiner et al., 2019), as well as structural improvements in cortical grey matter (Popescu et al., 2021), this also adds to the accumulating evidence for neuroplastic effects from TPS with corresponding behavioral changes.

#### **4.3 Decreases in visuo-constructive neuropsychological scores and graph theoretical measures indicate location specific effects of TPS**

As previously reported (Beisteiner et al., 2019), a location specific effect of TPS treatment was hypothesized due to overall increases in cognitive capacities, except for a specific decrease in visuo-constructive test scores. Crucially, brain areas central to these functions have been largely omitted during stimulation. The present results underline the decline in visuo-constructive abilities with a functional decrease in a VisNW. Historically, constructional apraxia was related to right hemispheric lesions (e.g. after right hemispheric stroke; Piercy et al., 1960). A modern perspective suggests that different aspects of visuo-constructive deficits relate to many different lesion loci and are not constrained in the right hemisphere (Gainotti & Trojano, 2018; Chechacz et al., 2014). In a lesion-mapping study with a large sample of stroke patients, Biesbroek et al. (2014) reported a variety of lesions in both hemispheres correlating with sub-scores of a complex figure copy task. Notably, these lesions were mainly located in the parietal and occipital parts of the brain, such as the AG R as well as right superior parietal lobe and middle occipital gyrus.

Constructional apraxia is not only present in patients with structural damage at these functionally relevant lesions, but is also one of the most common behavioral symptoms in

different dementias (Trojano & Gainotti, 2016). AD has been shown to involve large network disruptions over the entire brain as the disease progresses (Sendi et al., 2021). Typically, the symptoms are assigned either to problems in visual-spatial processing or to impairments in planning abilities, since constructional tasks, like copying a complex figure, requires strategy and can be considered a problem-solving task (Gainotti & Trojano, 2018). It has been shown that drawing tasks to test constructional deficits in patients can be a useful tool to monitor disease progression in AD (Binetti et al., 1998). There is a substantial amount of variability in the reported literature about the precise areas involved in visuo-constructive deficits. Arguably, this may often stem from different testing methods. In a functional imaging study using positron emission tomography, Förster et al. (2010) reported that hypoactivity in different posterior and parietal brain areas correlates with the difficulty in figure copying tasks. Such qualitative differences in test modalities can make it difficult to disentangle neural correlates of the diverse aspects in visuo-constructive impairments. Similarly, patient sample characteristics can produce variability in findings (Gainotti & Trojano, 2018). This factor can also be used to highlight different cognitive impairments involved in visuo-constructive disabilities. When comparing visuo-constructive impairments between patients with AD and frontotemporal dementia (FTD), Possin et al. (2011) could show that lower figure copy performance in AD was associated with spatial perception and attention, while in FTD it was associated with spatial planning and working memory. Correspondingly, low figure copy performance in the AD group correlated with right parietal cortex volume, while test scores FTD patients correlated with right DLPFC volume.

Serra et al. (2014) compared morphometric results between AD patients with or without constructional apraxia, which they grouped according to performance on a free-hand copying of drawings test. They could describe a network of parietal and occipital regions which showed a significant decrease in grey matter volume in AD patients with constructional apraxia. Because of this decline specific to an AD subgroup and the notable similarity with regions left out in the stimulation protocol in Beisteiner et al. (2019), this network was chosen for a sub-analysis. The Precun was excluded in the first network analysis, as it was the only ROI in the network from Serra et al. (2014) that received specific stimulation and potentially introduced a confounding effect.

Graph theoretical analysis of resting-state fMRI data showed significantly decreased GE in the AG R (Fig. 10; Tab. 2). GE is a measure for efficiency of information flow (Achard & Bullmore, 2007). The results presented here indicate functional deficiency in the AG R as

a part of the VisNW, as would be expected due to a continuing progression of the disease (Mondragón et al., 2021). Correspondingly, FIGURAL scores have also decreased after TPS stimulation, though slightly above the significance level (Fig. 6). Individual GE values for the AG R showed that the majority of individuals displayed either a decrease or no change after TPS intervention and only 2 patients had a slight increase (Fig. 11). Notably, the paired changes in individual GE and FIGURAL test scores showed the expected trend of a joint decline in GE and visuo-constructive performance (Fig. 12). One patient displayed a joint increase in GE and FIGURAL scores (along the expected relationship between connectivity changes and behavioral outcome) and only 3 patients had a visibly different response profile. Overall, the observed effects appear to be quite small, which is not surprising as only about 4 weeks have passed between measurements. Presumably, a functional decrease would have been stronger after a time of 3 months, when patients have also had the lowest FIGURAL test scores (Beisteiner et al., 2019).

As another result, including the Precun in the VisNW only slightly lessened the observed FC decline and the significant decrease in GE of the AG R remained (see VisNW+Precun, Tab. 2). It can be hypothesized that putative positive FC effects of TPS and negative effects of disease progression would cancel each other out. Together, this speaks to the validity of the observed functional decline: while a part of the stimulated Precun is included in the VisNW in Serra et al. (2014), it seems to not have a deciding functional influence on the network.

The pooled GE values of the VisNW and the majority of its nodes also correlated positively with the FIGURAL scores (Fig. 14). In contrast, parts of the network nodes of the VisNW+Precun also correlated with the (CERAD) CTS, showing a mixed behavior (notably the Precun correlated only with the CTS; Fig. 15). Separating the baseline and post stimulation also showed a positive correlation between the VisNW GE and FIGURAL scores (Fig. 16). While significance was not achieved, there was an observable trend. This indicates that the better the VisNW is functionally connected (both across the entire network or only with the AG R as a representative hub) the better the clinical visuo-constructive performance remains. Nevertheless, these results need to be interpreted with caution. Putatively, a larger sample size may fortify the positive correlation between FC values of the VisNW and FIGURAL scores, pre and post TPS.

#### 4.4 Evidence for neuromodulatory and location dependent effects of TPS

The results presented here are further supporting the case for neuromodulatory effects of TPS. Besides fMRI data strongly indicating off-line neuroplastic changes, immediate modulation in neuronal activity has also been observed after TPS application in ten human subjects. Stimulating the somatosensory cortex elicited somatosensory-evoked potentials (sham controlled) and a dosage dependent effect was also reported (Beisteiner et al., 2019). Disentangling the exact mechanisms of neuromodulation with sonication is still incomplete, however a number of models have been put forth, that also include important aspects for clinical translation. The most popular mechanism argues for a direct influence on membrane-bound mechanosensitive receptors and channels in neurons and support cells (Tyler, 2011). TFUS has been shown to induce calcium influx through mechanosensitive ion channels, which in turn elicits neural activation (Yoo et al., 2020). Recent results also suggest the likely possibility of glia cell mediated modulatory activity, through mechanical stimulation of membrane channels in astrocytes (Oh et al., 2020). Several reports have shown increases in BDNF after US stimulation in animal models (e.g. Fan et al., 2021; Zhang et al., 2019; Tufail et al., 2011). US can further induce cavitation effects and generate, for instance, bubbles or voids in cell membranes (Krasovitski et al., 2011). Another bio-effect observed in tFUS is hyperthermia, which has been shown to have inhibitory effects on motor neuron spiking in the medicinal leech (Collins et al., 2021). Importantly, increases in temperature seem to be dependent on longer sonication trains and  $I_{SPTA}$  values, i.e. a higher intensity over the course of US pulses (Darrow et al., 2019). Due to applying only single pressure pulses, TPS operates at a much lower intensity (max.  $I_{SPTA}$  of 0.1 W/cm<sup>2</sup>) and, therefore, poses no danger of tissue heating.

A further aspect of brain stimulation, which is vital for clinical translation, is inducing long-term, neuroplastic changes that go beyond immediate excitatory or inhibitory neuromodulation. Already 40 s of tFUS of brain structures in non-human primates have been shown to have prolonged activity effects, even after up to 2 hours have passed since intervention (Verhagen et al., 2019; Khalighinejad et al., 2020). Notably, TPS has shown increases in FC (Beisteiner et al., 2019) and also reduced grey matter atrophy in disease relevant brain areas (Popescu et al., 2021) after 2-4 weeks of intervention.

A clear advantage of US stimulation compared to e.g. current-based non-invasive brain stimulation methods is its high spatial resolution (Meng et al., 2021). While many developments have been made to increase spatial accuracy, there are still limitations (Cash et al., 2020). Problems especially occur in subjects with atypical brain morphology, e.g. due

to stroke, or more generally when attempting deep brain stimulation (Minjoli et al., 2017). In contrast, US stimulation can be tuned to have extremely precise local effects, even in deep tissue. Using 7 T MRI, Ai et al. (2018) demonstrated that tFUS can stimulate M1 thumb representation without inducing activity increase in neighboring M1 index or middle finger representations.

Verhagen et al. (2019) reported that not only the stimulated regions but also their closest connected neighboring areas show modulated activity patterns, and Folloni et al. (2019) reported a similar finding in deep brain structures, such as the amygdala and anterior cingulate cortex (both in non-human primates). This indicates an influence not only to the direct stimulation targets, but also indirectly to functionally connected areas. The current results suggest an indirect neuromodulatory effect of TPS intervention on two representative nodes of the SN and VMN (Fig. 7) without direct stimulation of these brain areas. While the extended DLPFC, the most widely used target in non-invasive brain stimulation for MDD, was included in the stimulated ROIs, a mechanistic model of the observed effect is not possible with this study. Cortico-thalamic-striatal FC (a brain circuit including nodes of the SN) has been shown to predict clinical outcome of TMS intervention in MDD patients (Salomons et al., 2014). TMS has been theorized to modulate this brain circuit and thereby influence the SN (Dunlop et al., 2017). A possible hypothesis for the current study is that TPS also acts upon this cortico-thalamic-striatal circuit and increases functional integrity within this circuit.

Complementary to this indirect modulation, the decrease in GE of the AG R as a node of a visuo-constructive network (Fig. 10) indicates a location-dependent effect of TPS. As already mentioned, Verhagen et al. (2019) reported that after stimulating, for instance, the secondary motor area in non-human primates, the global activity pattern changed proportional to the FC profile, meaning regions with a higher functional proximity (such as M1, superior parietal lobule or middle cingulate cortex) showed a relative increase in activity, while functionally more distant regions showed lower activity. Similarly, it can be argued that due to little or no overlap during TPS intervention with areas related to visuo-construction, a relative decrease in FC could be observed. Correspondingly, AD patients have shown a significant decrease in FIGURAL test scores after 3 months, which are in stark contrast to increases in the other CERAD subtest results (Beisteiner et al., 2019). This discrepancy also speaks to the validity of the functional and clinical outcomes: while there was no sham control for this study, the improvements in cognition and mood to-

gether with a specific functional and behavioral decline are promising evidence for a therapy-induced change instead of a placebo response.

#### **4.5 Limitations and conclusion**

A number of limitations have to be addressed. As already mentioned, the initial study included no sham-control and thus, results to be interpreted carefully. However, as already discussed, the results presented here strengthen the hypothesis of location-dependent effects of TPS and subsequently strengthen the foundation for the efficacy of TPS. Furthermore, the observed changes deviate from an expected placebo response (Ito et al., 2013). While all available patient data with completed fMRI measurements was included, the sample size was small. Nevertheless, it is still similar to recent related literature (e.g. Reznik et al., 2020; Cui et al., 2019). Future studies with larger sample sizes may be able to elucidate the observed variability in treatment responses, including 3 patients who responded atypically (Fig. 8). Concerning the generalizability in alleviating depressive symptoms, it has to be emphasized that this was an AD patient sample with mild depressive symptoms. While promising, TPS effects would need to be studied in an MDD patient sample for a stronger claim. The treatment duration may have been too short to induce stronger effects and subsequent studies may empirically tease out an ideal stimulation amount. Similarly, fMRI measurements were taken only at one time point after therapy and so not much is known about long-term functional changes. This would be especially interesting concerning the presented functional decreases in a VisNW, as behavioral decline has only reached significance 3 months after therapy.

TPS holds much promise as a clinical add-on therapy for AD, but also for other neurological and psychiatric diseases. These results give more evidence for stimulation-induced neuroplastic effects. Specifically, we could show promising signs on mitigating depressive symptoms with TPS and a potential functional basis for these changes. Further, while there are no sham controlled results at the moment, we fortified the claim for a location-dependent effect of TPS, which also makes a mere placebo effect improbable. Together, these are strong arguments to further explore the possibilities of TPS as a clinical add-on treatment.

## 5. References

- Abraha, I., Rimland, J. M., Trotta, F. M., Dell'Aquila, G., Cruz-Jentoft, A., Petrovic, M., Gudmundsson, A., Soiza, R., O'Mahony, D., Guaita, A., & Cherubini, A. (2017). Systematic review of systematic reviews of non-pharmacological interventions to treat behavioural disturbances in older patients with dementia. The SENATOR-OnTop series. *BMJ open*, *7*(3), e012759. <https://doi.org/10.1136/bmjopen-2016-012759>
- Achard, S., & Bullmore, E. (2007). Efficiency and cost of economical brain functional networks. *PLoS computational biology*, *3*(2), e17. <https://doi.org/10.1371/journal.pcbi.0030017>
- Agosta, F., Pievani, M., Geroldi, C., Copetti, M., Frisoni, G. B., & Filippi, M. (2012). Resting state fMRI in Alzheimer's disease: beyond the default mode network. *Neurobiology of aging*, *33*(8), 1564-1578.
- Ai, L., Bansal, P., Mueller, J. K., & Legon, W. (2018). Effects of transcranial focused ultrasound on human primary motor cortex using 7T fMRI: a pilot study. *BMC neuroscience*, *19*(1), 1-10.
- Andersson, J. L., Hutton, C., Ashburner, J., Turner, R., & Friston, K. (2001). Modeling geometric deformations in EPI time series. *Neuroimage*, *13*(5), 903-919.
- Ashburner, J., & Friston, K. J. (2005). Unified segmentation. *Neuroimage*, *26*(3), 839-851.
- Badhwar, A., Tam, A., Dansereau, C., Orban, P., Hoffstaedter, F., & Bellec, P. (2017). Resting-state network dysfunction in Alzheimer's disease: a systematic review and meta-analysis. *Alzheimer's & Dementia: Diagnosis, Assessment & Disease Monitoring*, *8*, 73-85.

- Badran, B. W., Caulfield, K. A., Stomberg-Firestein, S., Summers, P. M., Dowdle, L. T., Savoca, M., Li, X., Austelle, C. W., Short, E. B., Borckardt, J. J., Spivak, N., Bystritsky, A., & George, M. S. (2020). Sonication of the anterior thalamus with MRI-Guided transcranial focused ultrasound (tFUS) alters pain thresholds in healthy adults: A double-blind, sham-controlled study. *Brain stimulation*, *13*(6), 1805–1812. <https://doi.org/10.1016/j.brs.2020.10.007>
- Banerjee, S., Hellier, J., Romer, R., Dewey, M., Knapp, M., Ballard, C., ... & Lindsay, J. (2013). Study of the use of antidepressants for depression in dementia: the HTA-SADD trial-a multicentre, randomised, double-blind, placebo-controlled trial of the clinical effectiveness and cost-effectiveness of sertraline and mirtazapine. *Health technology assessment*, *17*(7).
- Behzadi, Y., Restom, K., Liou, J., & Liu, T. T. (2007). A component based noise correction method (CompCor) for BOLD and perfusion based fMRI. *NeuroImage*, *37*(1), 90–101. <https://doi.org/10.1016/j.neuroimage.2007.04.042>
- Beisteiner, R., Matt, E., Fan, C., Baldysiak, H., Schönfeld, M., Philippi Novak, T., Amini, A., Aslan, T., Reinecke, R., Lehrner, J., Weber, A., Reime, U., Goldenstedt, C., Marlinghaus, E., Hallett, M., & Lohse-Busch, H. (2019). Transcranial Pulse Stimulation with Ultrasound in Alzheimer's Disease-A New Navigated Focal Brain Therapy. *Advanced science (Weinheim, Baden-Wurttemberg, Germany)*, *7*(3), 1902583. <https://doi.org/10.1002/advs.201902583>
- Benoit, R. G., & Schacter, D. L. (2015). Specifying the core network supporting episodic simulation and episodic memory by activation likelihood estimation. *Neuropsychologia*, *75*, 450-457.
- Bergmann, T. O., Karabanov, A., Hartwigsen, G., Thielscher, A., & Siebner, H. R. (2016). Combining non-invasive transcranial brain stimulation with neuroimaging and electrophysiology: Current approaches and future perspectives. *NeuroImage*, *140*, 4–19.

- Biesbroek, J. M., van Zandvoort, M. J., Kuijf, H. J., Weaver, N. A., Kappelle, L. J., Vos, P. C., ... & Utrecht VCI Study Group. (2014). The anatomy of visuospatial construction revealed by lesion-symptom mapping. *Neuropsychologia*, *62*, 68-76.
- Binetti, G., Cappa, S. F., Magni, E., Padovani, A., Bianchetti, A., & Trabucchi, M. (1998). Visual and spatial perception in the early phase of Alzheimer's disease. *Neuropsychology*, *12*(1), 29.
- Brakowski, J., Spinelli, S., Dörig, N., Bosch, O. G., Manoliu, A., Holtforth, M. G., & Seifritz, E. (2017). Resting state brain network function in major depression—depression symptomatology, antidepressant treatment effects, future research. *Journal of Psychiatric Research*, *92*, 147-159.
- Cain, J. A., Visagan, S., Johnson, M. A., Crone, J., Blades, R., Spivak, N. M., ... & Monti, M. M. (2021a). Real time and delayed effects of subcortical low intensity focused ultrasound. *Scientific reports*, *11*(1), 1-14.
- Cain, J. A., Spivak, N. M., Coetzee, J. P., Crone, J. S., Johnson, M. A., Lutkenhoff, E. S., ... & Monti, M. M. (2021b). Ultrasonic thalamic stimulation in chronic disorders of consciousness. *Brain Stimulation: Basic, Translational, and Clinical Research in Neuromodulation*, *14*(2), 301-303.
- Camacho-Conde, J. A., Gonzalez-Bermudez, M., Carretero-Rey, M., & Khan, Z. U. (2021). Brain stimulation: a therapeutic approach for the treatment of neurological disorders. *CNS neuroscience & therapeutics*, [10.1111/cns.13769](https://doi.org/10.1111/cns.13769).
- Cash, R. F., Weigand, A., Zalesky, A., Siddiqi, S. H., Downar, J., Fitzgerald, P. B., & Fox, M. D. (2020). Using brain imaging to improve spatial targeting of transcranial magnetic stimulation for depression. *Biological psychiatry*.
- Caumo, W., Souza, I. C., Torres, I. L., Medeiros, L., Souza, A., Deitos, A., ... & Volz, M. S. (2012). Neurobiological effects of transcranial direct current stimulation: a review. *Frontiers in psychiatry*, *3*, 110.

- Chandler, M. J., Lacritz, L. H., Hynan, L. S., Barnard, H. D., Allen, G., Deschner, M., ... & Cullum, C. M. (2005). A total score for the CERAD neuropsychological battery. *Neurology*, *65*(1), 102-106.
- Chechlac, M., Novick, A., Rotshtein, P., Bickerton, W. L., Humphreys, G. W., & Demeyere, N. (2014). The neural substrates of drawing: a voxel-based morphometry analysis of constructional, hierarchical, and spatial representation deficits. *Journal of cognitive neuroscience*, *26*(12), 2701-2715.
- Ciric, R., Wolf, D. H., Power, J. D., Roalf, D. R., Baum, G. L., Ruparel, K., ... & Satterthwaite, T. D. (2017). Benchmarking of participant-level confound regression strategies for the control of motion artifact in studies of functional connectivity. *Neuroimage*, *154*, 174-187.
- Collins, M. N., Legon, W., & Mesce, K. A. (2021). The Inhibitory Thermal Effects of Focused Ultrasound on an Identified, Single Motoneuron. *eNeuro*, *8*(2), ENEURO.0514-20.2021.
- Cui, H., Ren, R., Lin, G., Zou, Y., Jiang, L., Wei, Z., Li, C., & Wang, G. (2019). Repetitive Transcranial Magnetic Stimulation Induced Hypoconnectivity Within the Default Mode Network Yields Cognitive Improvements in Amnesic Mild Cognitive Impairment: A Randomized Controlled Study. *Journal of Alzheimer's disease: JAD*, *69*(4), 1137–1151.
- Darrow, D. P., O'Brien, P., Richner, T. J., Netoff, T. I., & Ebbini, E. S. (2019). Reversible neuroinhibition by focused ultrasound is mediated by a thermal mechanism. *Brain stimulation*, *12*(6), 1439-1447.
- Dichter, G. S., Gibbs, D., & Smoski, M. J. (2015). A systematic review of relations between resting-state functional-MRI and treatment response in major depressive disorder. *Journal of affective disorders*, *172*, 8-17.
- Dunlop, K., Hanlon, C. A., & Downar, J. (2017). Noninvasive brain stimulation treatments for addiction and major depression. *Annals of the New York Academy of Sciences*, *1394*(1), 31.

- Ehrensperger, M. M., Berres, M., Taylor, K. I., & Monsch, A. U. (2010). Early detection of Alzheimer's disease with a total score of the German CERAD. *Journal of the International Neuropsychological Society*, *16*(5), 910-920.
- Fan, C. H., Wei, K. C., Chiu, N. H., Liao, E. C., Wang, H. C., Wu, R. Y., ... & Yeh, C. K. (2021). Sonogenetic-Based Neuromodulation for the Amelioration of Parkinson's Disease. *Nano Letters*, *21*(14), 5967-5976.
- Ferrarelli, F., & Phillips, M. L. (2021). Examining and Modulating Neural Circuits in Psychiatric Disorders With Transcranial Magnetic Stimulation and Electroencephalography: Present Practices and Future Developments. *The American journal of psychiatry*, *178*(5), 400–413.
- Fernandes, B. S., Molendijk, M. L., Köhler, C. A., Soares, J. C., Leite, C. M. G., Machado-Vieira, R., ... & Carvalho, A. F. (2015). Peripheral brain-derived neurotrophic factor (BDNF) as a biomarker in bipolar disorder: a meta-analysis of 52 studies. *BMC medicine*, *13*(1), 1-22.
- Folloni, D., Verhagen, L., Mars, R. B., Fouragnan, E., Constans, C., Aubry, J. F., ... & Sallet, J. (2019). Manipulation of subcortical and deep cortical activity in the primate brain using transcranial focused ultrasound stimulation. *Neuron*, *101*(6), 1109-1116.
- Förster, S., Teipel, S., Zach, C., Rominger, A., Cumming, P., la Fougere, C., ... & Bürger, K. (2010). FDG-PET mapping the brain substrates of visuo-constructive processing in Alzheimer's disease. *Journal of psychiatric research*, *44*(7), 462-469.
- Fox, M. D., Buckner, R. L., White, M. P., Greicius, M. D., & Pascual-Leone, A. (2012). Efficacy of transcranial magnetic stimulation targets for depression is related to intrinsic functional connectivity with the subgenual cingulate. *Biological psychiatry*, *72*(7), 595-603.
- Fry, F. J., Ades, H. W., & Fry, W. J. (1958). Production of reversible changes in the central nervous system by ultrasound. *Science*, *127*(3289), 83-84.

- Gainotti, G., & Trojano, L. (2018). Constructional apraxia. *Handbook of clinical neurology*, 151, 331-348.
- Galts, C. P., Bettio, L. E., Jewett, D. C., Yang, C. C., Brocardo, P. S., Rodrigues, A. L. S., ... & Gil-Mohapel, J. (2019). Depression in neurodegenerative diseases: common mechanisms and current treatment options. *Neuroscience & Biobehavioral Reviews*, 102, 56-84.
- Goebel, R. (2015). Revealing Brain Activity and White Matter Structure Using Functional and Diffusion-Weighted Magnetic Resonance Imaging. In C. Stipich (Ed.) *Clinical functional MRI: presurgical functional neuroimaging* (pp. 13-60). 2nd ed. Springer: Berlin Heidelberg.
- Guerra, A., Vicenzini, E., Cioffi, E., Colella, D., Cannavacciuolo, A., Pozzi, S., ... & Bologna, M. (2021). Effects of Transcranial Ultrasound Stimulation on Trigeminal Blink Reflex Excitability. *Brain sciences*, 11(5), 645.
- Hallett M. (2000). Transcranial magnetic stimulation and the human brain. *Nature*, 406(6792), 147–150.
- Hallquist, M. N., Hwang, K., & Luna, B. (2013). The nuisance of nuisance regression: spectral misspecification in a common approach to resting-state fMRI preprocessing reintroduces noise and obscures functional connectivity. *Neuroimage*, 82, 208-225.
- Henson, R. N. A., Buechel, C., Josephs, O., & Friston, K. J. (1999). The slice-timing problem in event-related fMRI. *NeuroImage*, 9, 125.
- Hohenfeld, C., Werner, C. J., & Reetz, K. (2018). Resting-state connectivity in neurodegenerative disorders: Is there potential for an imaging biomarker?. *NeuroImage. Clinical*, 18, 849–870.
- Ito, K., Corrigan, B., Romero, K., Anziano, R., Neville, J., Stephenson, D., & Lalonde, R. (2013). Understanding placebo responses in Alzheimer's disease clinical trials from the literature meta-data and CAMD database. *Journal of Alzheimer's disease : JAD*, 37(1), 173–183.

- Jeong, H., Im, J. J., Park, J. S., Na, S. H., Lee, W., Yoo, S. S., ... & Chung, Y. A. (2021). A pilot clinical study of low-intensity transcranial focused ultrasound in Alzheimer's disease. *Ultrasonography*.
- Khalighinejad, N., Bongioanni, A., Verhagen, L., Folloni, D., Attali, D., Aubry, J. F., Sallet, J., & Rushworth, M. (2020). A Basal Forebrain-Cingulate Circuit in Macaques Decides It Is Time to Act. *Neuron*, *105*(2), 370–384.e8.
- Kim, J., & Kim, Y. K. (2021). Crosstalk between Depression and Dementia with Resting-State fMRI Studies and Its Relationship with Cognitive Functioning. *Biomedicines*, *9*(1), 82.
- Koenigs, M., & Grafman, J. (2009). The functional neuroanatomy of depression: distinct roles for ventromedial and dorsolateral prefrontal cortex. *Behavioural brain research*, *201*(2), 239-243.
- Krasovitski, B., Frenkel, V., Shoham, S., & Kimmel, E. (2011). Intramembrane cavitation as a unifying mechanism for ultrasound-induced bioeffects. *Proceedings of the National Academy of Sciences*, *108*(8), 3258-3263.
- Lane, C. A., Hardy, J., & Schott, J. M. (2018). Alzheimer's disease. *European journal of neurology*.
- Lee, W., Chung, Y. A., Jung, Y., Song, I. U., & Yoo, S. S. (2016a). Simultaneous acoustic stimulation of human primary and secondary somatosensory cortices using transcranial focused ultrasound. *BMC neuroscience*, *17*(1), 1-11.
- Lee, W., Kim, H. C., Jung, Y., Chung, Y. A., Song, I. U., Lee, J. H., & Yoo, S. S. (2016b). Transcranial focused ultrasound stimulation of human primary visual cortex. *Scientific reports*, *6*(1), 1-12.
- Lee, W., Kim, H., Jung, Y., Song, I. U., Chung, Y. A., & Yoo, S. S. (2015). Image-guided transcranial focused ultrasound stimulates human primary somatosensory cortex. *Scientific reports*, *5*(1), 1-10.

- Legon, W., Ai, L., Bansal, P., & Mueller, J. K. (2018). Neuromodulation with single-element transcranial focused ultrasound in human thalamus. *Human brain mapping, 39*(5), 1995-2006.
- Legon, W., Sato, T. F., Opitz, A., Mueller, J., Barbour, A., Williams, A., & Tyler, W. J. (2014). Transcranial focused ultrasound modulates the activity of primary somatosensory cortex in humans. *Nature neuroscience, 17*(2), 322-329.
- Leinenga, G., Langton, C., Nisbet, R., & Götz, J. (2016). Ultrasound treatment of neurological diseases—current and emerging applications. *Nature Reviews Neurology, 12*(3), 161-174.
- Liston, C., Chen, A. C., Zebley, B. D., Drysdale, A. T., Gordon, R., Leuchter, B., Voss, H. U., Casey, B. J., Etkin, A., & Dubin, M. J. (2014). Default mode network mechanisms of transcranial magnetic stimulation in depression. *Biological psychiatry, 76*(7), 517–526.
- Lohse-Busch, H., Reime, U., & Falland, R. (2014). Symptomatic treatment of unresponsive wakefulness syndrome with transcranially focused extracorporeal shock waves. *NeuroRehabilitation, 35*(2), 235–244.
- Mammen, G., & Faulkner, G. (2013). Physical activity and the prevention of depression: a systematic review of prospective studies. *American journal of preventive medicine, 45*(5), 649-657.
- Meng, Y., Hynynen, K., & Lipsman, N. (2021). Applications of focused ultrasound in the brain: From thermoablation to drug delivery. *Nature Reviews Neurology, 17*(1), 7-22.
- Minjoli, S., Saturnino, G. B., Blicher, J. U., Stagg, C. J., Siebner, H. R., Antunes, A., & Thielscher, A. (2017). The impact of large structural brain changes in chronic stroke patients on the electric field caused by transcranial brain stimulation. *NeuroImage: Clinical, 15*, 106-117.

- Mondragón, J. D., Marapin, R., De Deyn, P. P., & Maurits, N. (2021). Short- and Long-Term Functional Connectivity Differences Associated with Alzheimer's Disease Progression. *Dementia and geriatric cognitive disorders extra*, *11*(3), 235–249.
- Monti, M. M., Schnakers, C., Korb, A. S., Bystritsky, A., & Vespa, P. M. (2016). Non-invasive ultrasonic thalamic stimulation in disorders of consciousness after severe brain injury: a first-in-man report. *Brain Stimul*, *9*(6), 940-941.
- Mueller, J., Legon, W., Opitz, A., Sato, T. F., & Tyler, W. J. (2014). Transcranial focused ultrasound modulates intrinsic and evoked EEG dynamics. *Brain stimulation*, *7*(6), 900-908.
- Nieto-Castanon, A. (2020). *Handbook of functional connectivity Magnetic Resonance Imaging methods in CONN*. Hilbert Press.
- Ogawa, S., Lee, T. M., Kay, A. R., & Tank, D. W. (1990). Brain magnetic resonance imaging with contrast dependent on blood oxygenation. *proceedings of the National Academy of Sciences*, *87*(24), 9868-9872.
- Oh, S. J., Lee, J. M., Kim, H. B., Lee, J., Han, S., Bae, J. Y., ... & Lee, C. J. (2020). Ultrasonic neuromodulation via astrocytic TRPA1. *Current Biology*, *30*(5), 948.
- Pascual-Leone, A., Rubio, B., Pallardó, F., & Catalá, M. D. (1996). Rapid-rate transcranial magnetic stimulation of left dorsolateral prefrontal cortex in drug-resistant depression. *The Lancet*, *348*(9022), 233-237.
- Perera, T., George, M., Grammer, G., Janicak, P., Pascual-leone, A., & Wirecki, T. (2016). TMS therapy for major depressive disorder: Evidence review and treatment recommendations for clinical practice. *Brain Stimulation*, *9*, 336-346.
- Pezzulo, G., Zorzi, M., & Corbetta, M. (2021). The secret life of predictive brains: what's spontaneous activity for?. *Trends in Cognitive Sciences*, *25*(9), 730–743.

- Piercy, M., Hecaen, H., & De Ajuriaguerra, J. (1960). Constructional apraxia associated with unilateral cerebral lesions—left and right sided cases compared. *Brain*, *83*(2), 225-242.
- Poldrack, R. A., Mumford, J. A., & Nichols, T. E. (2011). *Handbook of functional MRI data analysis*. Cambridge University Press.
- Popescu, T., Pernet, C., & Beisteiner, R. (2021). Transcranial ultrasound pulse stimulation reduces cortical atrophy in Alzheimer's patients: A follow-up study. *Alzheimer's & Dementia: Translational Research & Clinical Interventions*, *7*(1), e12121.
- Possin, K. L., Laluz, V. R., Alcantar, O. Z., Miller, B. L., & Kramer, J. H. (2011). Distinct neuro-anatomical substrates and cognitive mechanisms of figure copy performance in Alzheimer's disease and behavioral variant frontotemporal dementia. *Neuropsychologia*, *49*(1), 43-48.
- Reznik, S. J., Sanguinetti, J. L., Tyler, W. J., Daft, C., & Allen, J. J. (2020). A double-blind pilot study of transcranial ultrasound (TUS) as a five-day intervention: TUS mitigates worry among depressed participants. *Neurology, Psychiatry and Brain Research*, *37*, 60-66.
- Rovio, S., Kåreholt, I., Helkala, E. L., Viitanen, M., Winblad, B., Tuomilehto, J., ... & Kivipelto, M. (2005). Leisure-time physical activity at midlife and the risk of dementia and Alzheimer's disease. *The Lancet Neurology*, *4*(11), 705-711.
- Salomons, T. V., Dunlop, K., Kennedy, S. H., Flint, A., Geraci, J., Giacobbe, P., & Downar, J. (2014). Resting-state cortico-thalamic-striatal connectivity predicts response to dorsomedial prefrontal rTMS in major depressive disorder. *Neuropsychopharmacology*, *39*(2), 488–498.
- Sanguinetti, J. L., Hameroff, S., Smith, E. E., Sato, T., Daft, C. M., Tyler, W. J., & Allen, J. J. (2020). Transcranial focused ultrasound to the right prefrontal cortex improves mood and alters functional connectivity in humans. *Frontiers in human neuroscience*, *14*, 52.

- Scheltens, P., Blennow, K., Breteler, M. M., de Strooper, B., Frisoni, G. B., Salloway, S., & Van der Flier, W. M. (2016). Alzheimer's disease. *Lancet (Lond Engl)* 388: 505–517.
- Seeley, W. W. (2019). The salience network: a neural system for perceiving and responding to homeostatic demands. *Journal of Neuroscience*, 39(50), 9878-9882.
- Sendi, M., Zendeihrouh, E., Miller, R. L., Fu, Z., Du, Y., Liu, J., Mormino, E. C., Salat, D. H., & Calhoun, V. D. (2021). Alzheimer's Disease Projection From Normal to Mild Dementia Reflected in Functional Network Connectivity: A Longitudinal Study. *Frontiers in neural circuits*, 14, 593263.
- Serra, L., Fadda, L., Perri, R., Spanò, B., Marra, C., Castelli, D., ... & Bozzali, M. (2014). Constructional apraxia as a distinctive cognitive and structural brain feature of pre-senile Alzheimer's disease. *Journal of Alzheimer's Disease*, 38(2), 391-402.
- Siarkos, K. T., Katirtzoglou, E. A., & Politis, A. M. (2015). A review of pharmacological treatments for depression in Alzheimer's disease. *Journal of Alzheimer's Disease*, 48(1), 15-34.
- Soria Lopez, O. L., & Kuller, L. H. (2019). Epidemiology of aging and associated cognitive disorders: prevalence and incidence of Alzheimer's disease and other dementias. *Handbook of clinical neurology*, 167, 139-148.
- Spagnolo, P. A., Wang, H., Srivanitchapoom, P., Schwandt, M., Heilig, M., & Hallett, M. (2019). Lack of Target Engagement Following Low-Frequency Deep Transcranial Magnetic Stimulation of the Anterior Insula. *Neuromodulation: journal of the International Neuromodulation Society*, 22(8), 877–883.
- Sporns, O. (2011). *Networks of the Brain*. (1<sup>st</sup> Edition). Massachusetts Institute of Technology Press.
- Stern, Y. (2012). Cognitive reserve in ageing and Alzheimer's disease. *The Lancet Neurology*, 11(11), 1006-1012.

- Trojano, L., & Gainotti, G. (2016). Drawing disorders in Alzheimer's disease and other forms of dementia. *Journal of Alzheimer's Disease*, 53(1), 31-52.
- Tufail, Y., Matyushov, A., Baldwin, N., Tauchmann, M. L., Georges, J., Yoshihiro, A., ... & Tyler, W. J. (2010). Transcranial pulsed ultrasound stimulates intact brain circuits. *Neuron*, 66(5), 681-694.
- Tyler W. J. (2011). Noninvasive neuromodulation with ultrasound? A continuum mechanics hypothesis. *The Neuroscientist : a review journal bringing neurobiology, neurology and psychiatry*, 17(1), 25–36.
- Verhagen, L., Gallea, C., Folloni, D., Constans, C., Jensen, D. E., Ahnine, H., Roumazeilles, L., Santin, M., Ahmed, B., Lehericy, S., Klein-Flügge, M. C., Krug, K., Mars, R. B., Rushworth, M. F., Pouget, P., Aubry, J. F., & Sallet, J. (2019). Offline impact of transcranial focused ultrasound on cortical activation in primates. *eLife*, 8, e40541.
- Walsh, V., & Cowey, A. (2000). Transcranial magnetic stimulation and cognitive neuroscience. *Nature Reviews Neuroscience*, 1(1), 73-80.
- Whitfield-Gabrieli, S., & Nieto-Castanon, A. (2012). Conn: a functional connectivity toolbox for correlated and anticorrelated brain networks. *Brain connectivity*, 2(3), 125-141.
- Yarkoni, T., Poldrack, R. A., Nichols, T. E., Van Essen, D. C., & Wager, T. D. (2011). Large-scale automated synthesis of human functional neuroimaging data. *Nature methods*, 8(8), 665-670.
- Yoo, S., Mittelstein, D. R., Hurt, R., Lacroix, J., & Shapiro, M. G. (2020). Focused ultrasound excites neurons via mechanosensitive calcium accumulation and ion channel amplification. *bioRxiv*.
- Zhang, D., Li, H., Sun, J., Hu, W., Jin, W., Li, S., & Tong, S. (2019). Antidepressant-like effect of low-intensity transcranial ultrasound stimulation. *IEEE Transactions on Bio-medical Engineering*, 66(2), 411-420.

Zhang, J., Zhou, H., Yang, J., Jia, J., Niu, L., Sun, Z., ... & Wang, G. (2020). Low-intensity pulsed ultrasound ameliorates depression-like behaviors in a rat model of chronic unpredictable stress. *CNS Neuroscience & Therapeutics*, 27(2), 233-243.

Zhao, Q. F., Tan, L., Wang, H. F., Jiang, T., Tan, M. S., Tan, L., ... & Yu, J. T. (2016). The prevalence of neuropsychiatric symptoms in Alzheimer's disease: systematic review and meta-analysis. *Journal of affective disorders*, 190, 264-271.

## 6. List of abbreviations

AD	Alzheimer's disease
AG L / R	Angular gyrus (left / right)
AInsula R	Anterior insula (right)
BC	Betweenness centrality
BDI-II	Beck-Depression-Inventory
BDNF	Brain-derived neurotrophic factor
BOLD	Blood-oxygenated level dependent
Ct	Cost
CTS	Corrected total score
Dg	Degree
DLPFC	Dorsolateral prefrontal cortex
EEG	Electroencephalogram
FC	Functional connectivity
FDR	False discovery rate
fMRI	Functional magnetic resonance imaging
FOrb L	Frontal orbital cortex (left)
FTD	Frontotemporal dementia
GE	Global efficiency
ICC R	Intracalcarine cortex (right)
IFG R	Inferior frontal gyrus (right)
I <sub>SPTA</sub>	Spatial-peak-temporal-average intensity
MDD	Major depressive disorder
MMSE	Mini-mental state examination
MRI	Magnetic resonance imaging
MVPA	Multi-voxel pattern analysis
NIBS	Non-invasive brain stimulation
PCA	Principal component analysis
PCC	Posterior cingulate cortex
pMTG R	Posterior medial temporal gyrus (right)
Precun	Precuneus
QC	Quality control
ROI	Region of interest

SD	Standard deviation
sgACC	subgenual anterior cingulate cortex
SN	Saliience Network
tDCS	Transcranial direct current stimulation
tFUS	Transcranial focused ultrasound
TMS	Transcranial magnetic stimulation
toFusC R	Temporo-occipital fusiform cortex (right)
TPS	Transcranial pulse stimulation
US	Ultrasound
VisNW (+Precun)	Visuo-constructive network (+ precuneus)
VMN	Ventromedial Network

## 7. List of Figures and Tables

Figure 1: Diagram of the study design

Figure 2: Example of outlier detection (subject 18).

Figure 3: FC distribution before and after denoising procedures.

Figure 4: QC-FC correlation distribution before and after denoising.

Figure 5: Improvement of depression score (Beck Depression Inventory, BDI-II) after TPS stimulation.

Figure 6: FIGURAL test scores show a tendency to decline after TPS therapy.

Figure 7: Functional connectivity changes following TPS treatment in ROI-to-ROI connectivity analysis.

Figure 8: Individual FC values between left frontal orbital cortex (FOrb L) and right anterior insula (AInsula R) at baseline and post stimulation sessions.

Figure 9: Functional connectivity map derived from Neurosynth (Yarkoni et al., 2011) shows negative connectivity between FOrb L and AInsula R.

Figure 10: Visuo-constructive network shows reduced global efficiency (GE) post vs. pre stimulation.

Figure 11: Individual global efficiency (GE) values for the right angular gyrus (AG R) at baseline and post stimulation session.

Figure 12: Decrease in global efficiency (GE) in the right angular gyrus (AG R) corresponds to a decline in visuo-constructive test scores.

Figure 13: Functional connectivity post stimulation correlates with depression symptom improvements.

Figure 14: Global efficiency (GE) for visuo-constructive network (without precuneus) correlates with (CERAD) FIGURAL scores.

Figure 15: Global efficiency (GE) for visuo-constructive network (including precuneus) correlates with (CERAD) FIGURAL and CTS scores.

Figure 16: Global efficiency (GE) of visuo-constructive network and (CERAD) FIGURAL scores at baseline and post TPS intervention show a joint trend.

Table 1: List of ROIs for graph analysis of a visuo-constructive network

Table 2: Graph measures post vs. pre stimulation for two visuo-constructive networks